LATE TO MIDDLE JURASSIC SOURCE FACIES AND QUALITY VARIATIONS, SOUTH VIKING GRABEN, NORTH SEA

H. Justwan*[1], B. Dahl[1], G.H. Isaksen[2] and I. Meisingset[3]

Source facies and quality of the Late to Middle Jurassic source rock system in the South Viking Graben between 58°N and 60°15'N are highly variable both regionally and stratigraphically. In order to assess the degree of variability and to create a model of source rock quality and potential, isochore maps of the syn- and post-rift sections of the Upper Jurassic Draupne Formation and underlying Heather Formation were generated from seismic and well data, and maturity-corrected Rock-Eval data were used to generate quantitative maps of oil and gas potential. The thin post-rift section at the top of the Draupne Formation is a rich oil-prone source, while the up to 1,600 m thick syn-rift section contains a mixture of Type III and Type II material with substantial amounts of gas-prone and inert organic matter. The Heather Formation, which reaches modelled thicknesses of up to 930 m, is a lean source and is generally gas-prone.

Detailed analyses and interpretations of biomarker and isotopic characteristics support this upward increase in oil-prone Type II material. The analytical parameters include increasing relative amounts of C_{27} regular steranes; decreasing ratios of C_{30} moretane relative to C_{30} hopane; and an increasing predominance of short chain n-alkanes and progressively lighter isotopic values for saturate and aromatic fractions of source rock extracts. In addition, increasing amounts of 17α(H),21β(H)-28,30-bisnorhopane and decreasing amounts of C_{34} homohopanes relative to C_{35} homohopanes, as well as decreasing Pr/Ph ratios, suggest a general decrease in oxygenation upwards. Maps of average Pr/Ph ratios for the syn- and post-rift Draupne Formation and for the Heather Formation are consistent with permanent water column stratification and gradual ascent of the O_2:H_2S interface from the Callovian to the Ryazanian.

Interpretation of oil and gas potential maps, molecular parameters and estimates of sediment accumulation rates in combination suggest that the source facies of the upper, post-rift Draupne Formation is controlled by widespread anoxia, reduced siliciclastic dilution and reduced input of gas-prone organic and inert material; by contrast, the potential of the lower, syn-rift Draupne Formation is strongly controlled by dilution by gas-prone and inert organic matter resulting from mass flows and also by varying degrees of oxygenation. The oil and gas potential of the Heather Formation is mainly controlled by the degree of oxygenation and siliciclastic dilution.

INTRODUCTION

Source facies and quality of Jurassic source rocks in the Viking Graben vary both laterally and vertically (Huc *et al*., 1985; Isaksen and Ledje, 2001; Kubala *et al*., 2003; Justwan and Dahl, 2005). In the area between 58º N and 60º15' N in the Norwegian South Viking Graben, major differences can be observed between syn- and post-rift sections of the Draupne Formation (Justwan and Dahl, 2005). As more data concerning Jurassic source rocks in the mature exploration area of the South Viking Graben become available, it is becoming evident that source facies distribution can no longer be explained by simple models and that it is controlled by numerous factors. The new data has enabled us to construct a more

[1]Department of Earth Science, University of Bergen, Allegaten 41, 5007 Bergen, Norway.
[2] ExxonMobil Exploration Company, 233 Benmar, Houston, Texas 77210, USA.
[3] Aker Kvaerner Geo AS, PO Box 242, Lilleaker, 0216 Oslo, Norway.
*corresponding author, email: holger.justwan@geo.uib.no

reliable model of source rock distribution, potential and quality than was previously possible. We have focussed on the Upper Jurassic source interval because only a small amount of new data on the Middle Jurassic source rocks in the study area was available.

This paper forms the first part of a larger study of the petroleum system in the South Viking Graben which will also include an oil-source correlation study and a basin modelling project. The objectives of the present paper are threefold. The first aim is to produce maps of the thickness and quality of the Upper Jurassic source rock section which can be used in basin modelling. Much attention in recent basin modelling projects has been given to kinetic parameters (e.g. Dieckmann *et al*., 2004) and phase predictions (e.g. di Primio, 2002), while the issue of source rock variability as an important input parameter is rarely addressed. We hope to shed light on this important aspect of the petroleum systems of the South Viking Graben by presenting quantitative maps of the oil and gas potential in the area. The second objective of this study is to gain a detailed knowledge of variations in source rock quality (including molecular properties) which will later be used in an oil-source correlation study within the South Viking Graben. Finally, we attempt to explain the development of source facies and oil and gas potential in the area in terms of basin development through time.

GEOLOGICAL SETTING

Evolution of the South Viking Graben

The present-day structural configuration of the study area (Fig. 1) was inherited from two major extensional phases in the Permo-Triassic and the Late Jurassic (Ziegler, 1992). Permo-Triassic extension was more pronounced in the Stord Basin on the eastern margin of the study area, while Jurassic extension mainly affected the Viking Graben in the west and left the Stord Basin largely unaffected (Faerseth, 1996). The South Viking Graben is asymmetric; it is bound by the East Shetland Platform to the west, and steps up to the east with numerous fault blocks (Fig. 1) forming the Gudrun and Sleipner terraces (Cockings *et al*., 1992; Sneider *et al*., 1995). The Utsira High, which was a positive feature at least as early as the Permian (Hanslien, 1987), together with the Ling High constitute the eastern boundary of the graben. The oldest sediments encountered in the area are of Permian age (Isaksen *et al*., 2002) and are overlain by Triassic continental siliciclastics (Fisher and Mudge, 1998). Marine sediments of the Lower Jurassic Dunlin Group were deposited during a rise in sea level (Skarpnes *et al*., 1980), but are sparsely preserved south of 59°N. The Brent delta developed in the northern half of the study area in response to regional doming during the Middle Jurassic. Its sediments pass transgressively southwards into the coastal plain deposits of the Sleipner Formation and the shallow-marine to coastal deposits of the Hugin Formation. Middle Jurassic sandstones form important reservoir intervals in the area, while the coals and coaly shales are source rocks for gas and volatile oils (Isaksen *et al*., 1998). The organic rich oil- and gas-prone shales of the Heather and Draupne Formations were deposited during a sea-level rise in the Late Jurassic. Intra-Heather and Draupne Formation sandstones also act as reservoirs in the study area, and are best developed along the western margin of the South Viking Graben in the UK Sector. Following Late Jurassic rifting, there followed a period of tectonic quiescence and subsequent uplift and erosion of the East Shetland Platform, resulting in the deposition of submarine fan sandstones of Paleocene to Eocene age which include important reservoir intervals. Continued subsidence with occasional phases of uplift accompanied by the resulting supply of sediments from the west resulted in an extensive post-Eocene sedimentary section (Gregersen *et al*., 1997).

The Jurassic source rock system in the South Viking Graben

The Upper Jurassic Draupne Formation and stratigraphic equivalents are the major source rocks in the North Sea and have been subject of numerous studies (e.g. Barnard and Cooper, 1981; Goff, 1983; Cooper and Barnard, 1984; Doré *et al*., 1985; Field, 1985; Northam, 1985; Cooper *et al*., 1993; Cornford, 1998; Kubala *et al*., 2003). In addition, the underlying Heather Formation together with Middle Jurassic units also have potential for oil and gas generation (Cooper and Barnard, 1984; Field, 1985; Cornford, 1998; Isaksen *et al*., 1998; Isaksen *et al*., 2002). In the following paragraphs, we summarise previous studies concerning Jurassic source rocks in the study area.

The mid-Jurassic Sleipner and Hugin Formations (Fig. 2) were deposited in a coastal plain to offshore marine setting. The Sleipner Formation, which is up to 500 m thick (Husmo *et al*., 2003), consists mainly of fluvio-deltaic siliciclastics including coals and coaly shales, and ranges in age from Bathonian to earliest Oxfordian on the margins of the Utsira High (Vollset and Doré, 1984; Cockings *et al*., 1992). It is transgressively overlain by the Hugin Formation of latest Bathonian to Early Oxfordian age (Cockings *et al*., 1992; Husmo *et al*., 2003) which comprises nearshore shallow-marine sandstones and fluviodeltaic sediments including coals and coaly shales (Vollset and Doré, 1984). These Middle Jurassic coals and coaly shales have the potential to generate gas and volatile oil (Isaksen *et al*., 1998), and exhibit

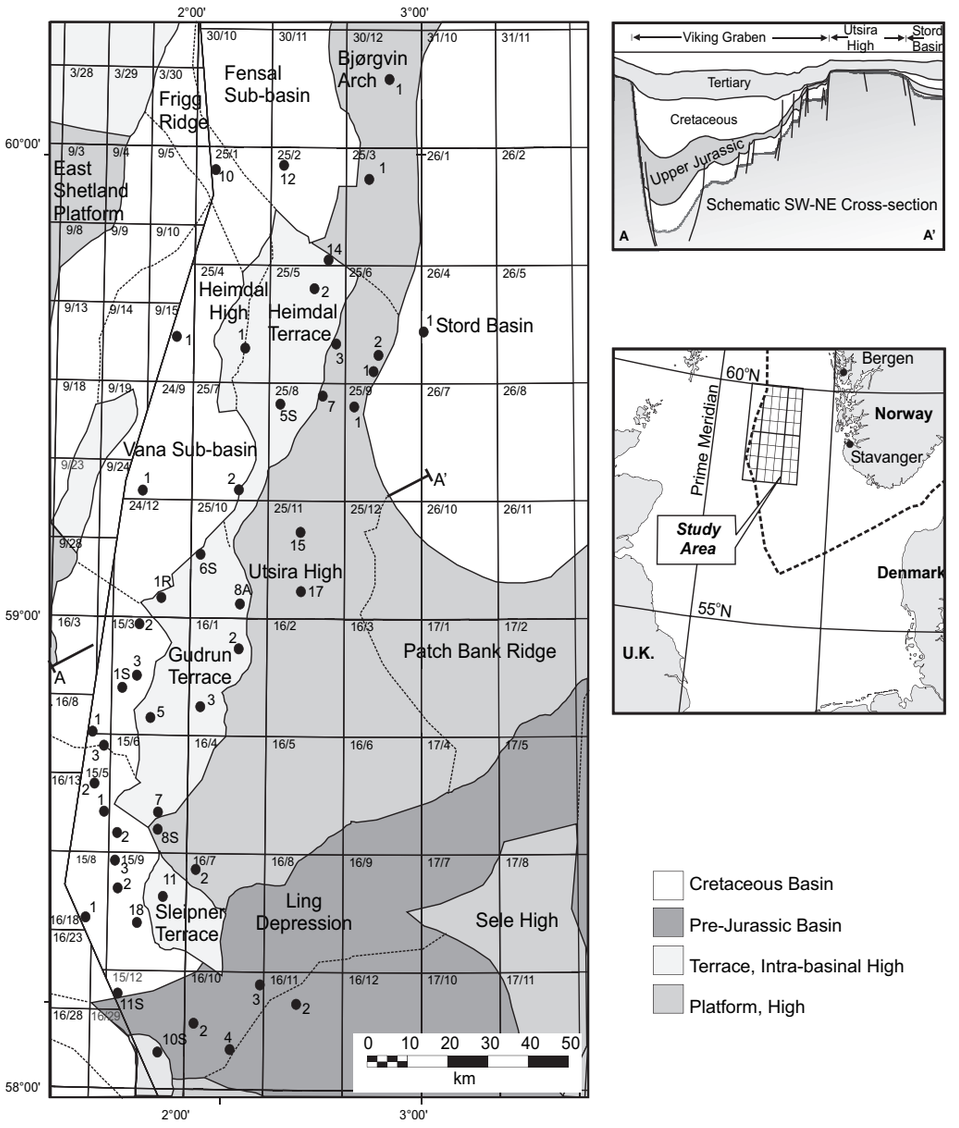

Fig. 1. General map of the South Viking Graben showing major structural elements (after Norwegian Petroleum Directorate, 2005) and the location of the wells used in quantitative source rock mapping. The schematic SW-NE cross-section (after Isaksen and Ledje, 2001) displays the structure of the South Viking Graben, the flanking highs and the adjacent Stord Basin (line of section A-A' in main map). The location of the study area in the North Sea is shown in the overview map (lower right).

TOC values of up to 80 wt % and Hydrogen Indices up to 400 g HC/kg C_{org} (Isaksen *et al*., 2002). Shales and grey silty mudstones of the Callovian to Oxfordian Heather Formation have average TOC values up to 4% (Goff, 1983; Cooper and Barnard, 1984; Field, 1985; Thomas *et al*., 1985). It is generally thought that this formation is a lean dry gas source, although it shows large variations in source potential and has good hydrocarbon potential in some small sub-basins (Cooper and Barnard, 1984; Field, 1985; Thomas *et al*., 1985; Scotchman, 1991; Gormly *et al*., 1994; Isaksen *et al*., 2002). Thomas *et al*. (1985) described a widespread basal-Heather "hot shale" deposited under dysoxic to anoxic conditions beneath a stratified water column, whose deposition was terminated by increasing oxygenation accompanying a progressive transgression.

The Heather Formation is diachronously overlain by the Oxfordian to Ryazanian (Kimmeridge Clay Equivalent) Draupne Formation (Vollset and Doré, 1984) (Fig. 2). Various depositional models for this unit have been put forward (e.g. Hallam and Bradshaw, 1979; Tyson *et al*., 1979; Demaison and Moore, 1980; Parrish and Curtis, 1982; Oschmann, 1988; Miller, 1990). The well studied onshore outcrops are however not easily comparable in age or facies with the offshore equivalent (Wignall, 1994). It is generally agreed that deposition of the offshore

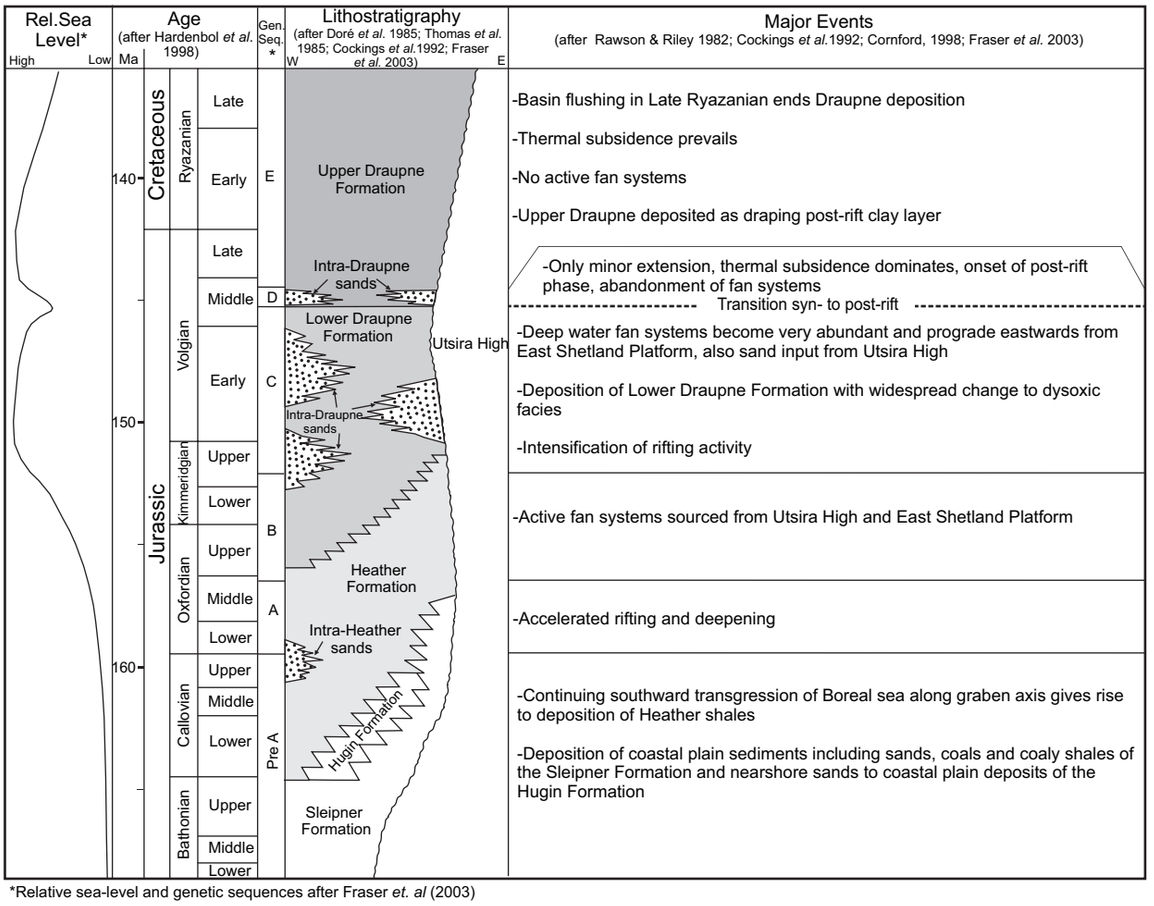

*Relative sea-level and genetic sequences after Fraser *et. al* (2003)

Fig. 2. General stratigraphic chart of the Upper to Middle Jurassic succession in the South Viking Graben with a summary of the major tectonic and depositional events. The Oxfordian to Kimmeridgian Draupne Formation can be divided into an upper post-rift section including genetic sequences D and E (Fraser *et al.*, 2003) and a lower syn-rift section. The Draupne and Heather Formation contain a series of sands sourced from the flanking highs, the East Shetland Platform and the Utsira High.

Kimmeridge Clay occurred in a shallow sea with anoxic bottom waters (Cornford, 1998), although the degree of oxygenation appears to decrease from the lower to the upper Draupne Formation (Thomas *et al*., 1985; Justwan and Dahl, 2005). The Draupne Formation has TOC up to 12 wt% (Thomas *et al*., 1985) and Hydrogen Indices which are well over 600 g HC/kg C_{org}. However, the formation has large lateral and vertical variations in source quality (Field, 1985; Huc *et al*., 1985; Scotchman, 1991; Cooper *et al*., 1993; Isaksen and Ledje, 2001; Kubala *et al*. 2003), especially in the narrow South Viking Graben whose fringing land areas were the source of terrestrial organic matter. It has been observed not only that the terrestrial contribution decreases upwards (Huc *et al*., 1985), but also that there is a distinct difference in source facies and potential between the upper and lower parts of the formation. Thus, the upper section has better source quality and richness, while the lower part has a higher content of Type III kerogen (Field, 1985; Huc *et al*., 1985; Isaksen and Ledje, 2001; Isaksen *et al*., 2002; Kubala *et al*., 2003). The upper and lower parts of the Draupne Formation were therefore considered separately in the present study.

In general, these sections correspond to post- and syn-rift successions although the identification of these intervals is difficult in the study area (Gabrielsen *et al*., 2001; see also Rawson and Riley, 1982; and Rattey and Hayward, 1993). For this study, the base of the J70 sequence of Rattey and Hayward (1993) was chosen as the base of the post-rift section. This corresponds to the base of genetic sequence D of Middle Volgian age of Fraser *et al*. (2003), and the Ti5 sequence boundary of Jacquin *et al*. (1998) (Fig. 2). Gamma-ray log pattern and geochemical data were utilized in addition (see below). The lowermost section of the syn-rift lower Draupne Formation was deposited during intensifying rift activity and rising relative sea level (genetic sequence B, see Fig. 2) with fan systems shedding sands from the surrounding highs. The South Viking Graben contains a series of these basinward-thinning and -fining sandy

wedges of Kimmeridgian to Volgian age (Thomas *et al*., 1985; Sneider *et al*., 1995; Underhill, 1998; Isaksen and Ledje, 2001) which are interpreted to be proximal deep-water slope apron complexes sourced from the East Shetland Platform and the Utsira High (Underhill, 1998; Fraser *et al*., 2003). They contain large amounts of reworked terrestrial organic matter (Cooper *et al*., 1993; Isaksen and Ledje, 2001; Justwan and Dahl, 2005). Rifting intensified in the Early Volgian and widespread dysoxic conditions were established (Fraser *et al*., 2003). A regressive episode followed in the Middle Volgian while fan deposition continued.

The upper Draupne Formation represents a clay layer deposited during thermal subsidence after the cessation of rifting. Its lowermost section was deposited during the late Middle Volgian when fan systems became less common. The uppermost section, corresponding to genetic sequence E of Fraser *et al*. (2003), does not show the influence of fans (Fig.2). Mass flows from surrounding highs therefore had much less of an influence in the upper Draupne Formation.

In general, areas surrounding highs and close to the palaeo-shoreline were dominated by the deposition of Type III and IV organic matter (Thomas *et al*., 1985; Cooper *et al*., 1993; Kubala *et al*., 2003). The deep, basinal sections are richest in Type II organic matter (Thomas *et al*., 1985; Miller, 1990; Cornford, 1998), with a typical concentric, outward-decreasing TOC distribution (Huc, 1988; Cooper *et al*., 1993). Although the basinal sections are generally oil prone, they can potentially contain large amounts of inertinite transported by mass flow processes (Tyson, 1989; Thomas *et al*., 1985). Below, using recently-acquired data, we investigate if these general assumptions are still applicable to the South Viking Graben, and attempt to determine the controls on the distribution of organic facies in this area.

SAMPLES, DATA, ANALYTICAL METHODS

A large Rock-Eval database was available comprising samples from 47 wells in the study area, of which eight where analysed during this project using a *Vinci Technologies Rock-Eval 6* in bulk rock mode. The remaining data is derived from geochemical service reports publicly available from the Norwegian Petroleum Directorate or were provided by Esso Norway. Cuttings provided by the Norwegian Petroleum Directorate for this project from the source rock sections of eight wells were analysed by gas chromatography (GC) and gas chromatography-mass spectrometry (GC-MS). In addition, the isotopic composition of 15 samples from well *15/9-18* were analysed. Vitrinite reflectance data (36 wells), GC and GC-MS data (26 wells) and isotope data (21 wells) obtained from the Norwegian Petroleum Directorate, Esso Exploration and Production A/S Norway or previous projects at the University of Bergen were also used.

Solvent extraction was carried out with a *SOXTEC System HT2 1045* extraction unit on washed, crushed and ground cutting samples with dichloromethane/methanol (93:7) as solvent. The asphaltene fraction of all samples was precipitated by adding an excess amount of *n*-pentane, following the procedure suggested in Weiss *et al*. (2000). For GC, GC-MS and isotope analysis, preparative group-type separation of the maltene fraction was carried out using medium pressure liquid chromatography (MPLC) following methods modified from Radke *et al*. (1980). The carbon isotopic analysis of the saturate and aromatic fractions was carried out on a *Carlo Erba NA 1500* elementary analyser and a *Finnigan MAT Delta E* online mass spectrometer. All results are reported against PDB. The saturate hydrocarbon fraction of extracts of all source rock samples from wells *15/9-18*, *25/5-5*, *25/7-2*, *16/7-2* and *25/1-10* were analysed using a *Hewlett Packard GC-MSD*, consisting of a *HP 6890 GC Plus*, a *HP 5973* Mass Selective Detector operating in SIM mode at the University of Bergen. The GC unit was equipped with two *HP 19091Z-105* HP-1 methyl siloxane columns each of 50 m nominal length, 200 µm nominal diameter and 0.33 µm nominal film thickness. The oven's initial temperature was 50°C and increased regularly during 20 minutes to an end temperature of 310°C until 80 minutes. Helium was used as the carrier gas. The temperature of the FID was 320°C and the hydrogen flow was 40 ml/min, while the airflow was held at 400 ml/min.

The saturate hydrocarbon fractions of samples from wells *15/3-3*, *15/3-5* and *16/1-2* (location see Fig.1) were analysed on the same system, but using two *HP 19091J-102 HP-5* 5% phenyl methyl siloxane columns of 25 m nominal length. The oven's initial temperature was 70°C, increased during 20 minutes to an end temperature of 310°C until 60 minutes, and the airflow was held at 450 ml/min. GC and GCMS ratios were calculated from measured peak heights. For all analyses performed, standards were run every tenth sample to ensure analytical quality and comparability of results.

RESULTS AND DISCUSSION

Thickness, areal extent and accumulation rates of the Upper Jurassic source rock intervals

For basin modelling, the quality and potential of the source rock as well as the thickness of the respective source intervals should be investigated. To produce isochore maps of the upper Draupne, lower Draupne

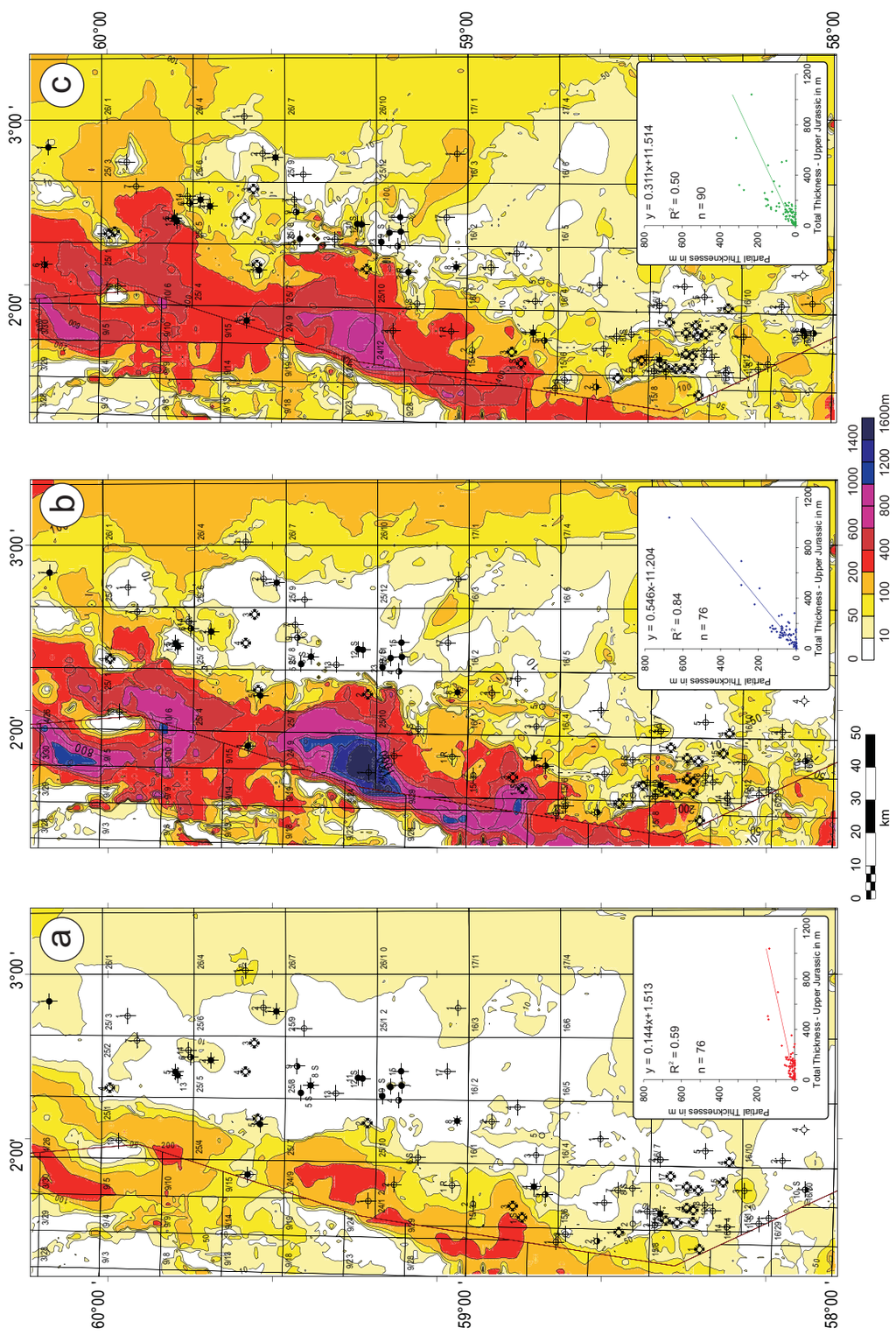

Fig. 3. Isochore maps of (a) the upper Draupne, (b) the lower Draupne and (c) the Heather Formation. The maps were derived from an Upper Jurassic thickness map between the near base-Cretaceous and the top-Middle Jurassic surface which was split using well data and the statistical relationship between the total Upper Jurassic thickness and the partial thicknesses of the respective units from well data (see inset graphs).

and Heather Formation, a pragmatic statistical approach was chosen because the intra-Upper Jurassic surfaces are not discernable on seismic sections. This method is very coarse, but gives a general idea about the distribution of the analysed source rock sections and their thicknesses. The information used comprised an Upper Jurassic thickness map which was based on the near base-Cretaceous and top-Middle Jurassic surfaces, as well as data from 90 well penetrations. In this process, linear regression analysis was performed to investigate the statistical relationship between the total thickness of the Upper Jurassic succession and the partial thicknesses of the upper and lower Draupne and Heather Formations (Fig. 3, insets).

The total Upper Jurassic thickness and the partial thickness of the lower Draupne Formation are strongly correlated ($R^2 = 0.84$) (Fig. 3b, insets), while total and partial thicknesses for the upper Draupne and the Heather Formation have lower correlation coefficients of 0.59 and 0.50 respectively (Fig. 3a,c, inset). Based on the observed statistical relationships (equations see Fig. 3, inset), the total Upper Jurassic isochore was subdivided into three sections, corresponding to the upper and lower Draupne and Heather Formations.

The maximum modelled thickness of the Heather Formation is approximately 930 m in the deepest parts of the graben, while the maximum observed thickness is 315 m in well *24/12-2* (Fig. 3c). The thickness decreases to the east and although the Heather Formation does not cover the entire Utsira High area, it is the most widespread of the three analysed source rock units. The lower Draupne Formation is up to about 1,600 m thick in depocentres in the graben, with a maximum observed thickness of 671 m in well *15/3-1S* and decreases rapidly in thickness towards the Utsira High in the east (Fig. 3b). The upper Draupne Formation is considerably thinner, with thicknesses of up to approximately 330 m and a maximum observed thickness of 142 m in well *15/3-3* (Fig. 3a); it appears to fill relief in the graben as a draping clay layer deposited after the cessation of rifting (Fig. 3a). The Utsira High remained partly emergent during the deposition of the upper Draupne Formation (Fraser *et al*., 2003) which is less than 10 m thick on the high.

Average compacted linear sediment accumulation rates were determined for the studied section from well data using Esso's proprietary sequence stratigraphic framework. While hiatuses are included, the mass flow sand units have been removed because they represent very rapid events which would introduce additional error, increasing the accumulation rates. The accumulation rate in the Heather Formation ranges from 1 m/Ma to over 50 m/Ma, with an average value of around 20 m/Ma in the analysed wells. Linear sediment accumulation rates in the lower Draupne Formation are between 1 and 47 m/Ma with an average of 11.7 m/Ma. The upper Draupne Formation appears sediment starved and has even lower accumulation rates, reaching a maximum of 20m/Ma in the deep graben and around 1m/Ma for the condensed sections on the Utsira High, with an average of only 7m/Ma. Sediment starvation in the mid-Volgian to Ryazanian has also been observed in the Danish Central Graben (Ineson *et al*., 2003).

Similar accumulation rates were reported by Miller (1990) for the Kimmeridge Clay Equivalent in the Northern North Sea. These values are, however, significantly lower than the 40 to 100 m/Ma for the Kimmeridge Clay of the Wessex Basin (Tyson, 2004) which is the approximate time-equivalent of the offshore lower Draupne Formation. Considering the much larger thicknesses in the undrilled sections of the South Viking Graben not used in the calculations above, values in the South Viking Graben might however approach those of Tyson (2004).

Source rock thermal maturity and hydrocarbon generation

The analysed sections exhibit a wide range of thermal maturities as a function of burial depth, ranging from immature on the highs to late mature in the deeper parts of the graben. Maturity determination is strongly dependent on kerogen type (Tissot and Welte, 1984; Waples and Marzi, 1998; Kubala *et al*., 2003). Various studies (e.g. Huc *et al*., 1985; Isaksen and Ledje, 2001; Kubala *et al*., 2003; Justwan and Dahl, 2005) have shown that the Draupne and Heather Formation contain variable mixtures of terrestrial and marine organic matter. Source rocks in the Middle Jurassic Vestland Group, which were deposited in a generally terrestrial environment, are dominated by Type III kerogen. Due to these variations, the source rock thermal maturity was determined for each section separately. The onset of generation was determined from depth plots of the Hydrogen Index (HI), Bitumen Index (BI=S1/TOC*100) and Production Index (PI=S1/(S1+S2)), and cross-checked with high-quality vitrinite reflectance and Rock-Eval T_{max} values (Fig. 4a-e).

The HI versus depth plot (Fig. 4a) is a good indicator for the onset of generation (Petersen *et al*., 2002; Kubala *et al*., 2003; Justwan and Dahl, 2005). In the study area, within the Upper Jurassic, a decline in the HI trend at around 3,500 m coincides with vitrinite reflectance values of 0.6% and T_{max} values of 435 ºC, all indicating the onset of hydrocarbon generation. Baird (1986) determined the onset of generation to be at 3,340 m, while Isaksen and Ledje (2001) proposed a depth of 3,400 m and Kubala *et al*. (2003) a depth of 3,500 m for

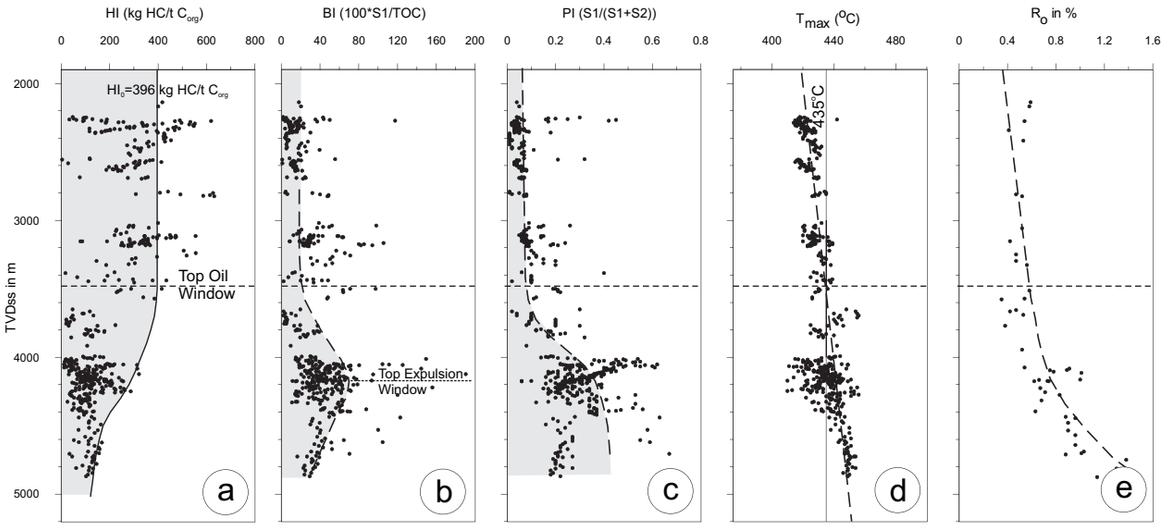

Fig. 4. Depth plots of (a) Hydrogen Index (HI), (b) Bitumen Index (BI), (c) Production Index (PI), (d) Rock-Eval T_{max} and (e) vitrinite reflectance for the lower Draupne Formation. These depth plots were used to determine the transformation ratio which was then used to restore TOC and Hydrogen Index to their prematuration values.

the same area. The onset of hydrocarbon generation appears to be slightly deeper at around 3,800 m for the Middle Jurassic Vestland Group. Rock-Eval T_{max} and vitrinite reflectance (Fig. 4d, e) are in good agreement with these observations and confirm a depth of 3,500 m for the top of the oil window in the Upper Jurassic section.

Peak oil generation, or onset of expulsion (Petersen *et al*., 2002), was estimated to occur at a depth of around 4,100 m for the lower Draupne Formation (Fig. 4b). Expulsion occurs at a slightly shallower level for the upper Draupne Formation (around 4,000 m) and at around 4,200 m for the Heather Formation (not shown).

Based on thermal maturity data, the original source rock properties were restored to compensate for maturity related differences. The empirical method used here is based on studies by Espitalié *et al*. (1987) and Justwan and Dahl (2005), and uses depth plots of HI, PI and BI to establish regional generation curves which are then used to restore the original source rock properties (TOC^0, $S2^0$ and resulting HI^0 from Rock-Eval). The data set for the respective source intervals was filtered to remove contaminated samples. The large spread of data in the immature range above 3,500 m, which reflects the fact that the data originates from multiple wells, makes the determination of the original pre-maturation Hydrogen Index (HI_0) difficult. HI_0 was taken as the 3rd quartile value of the HI distribution between 0 and 3,500 m — for example, 396 g HC/kg C_{org} for the lower Draupne Formation. This choice is in good agreement with the shape and curvature of the trend-line which is an envelope in the mature section. The construction of trend-lines for the upper and lower Draupne Formation and the Heather Formation was made possible by the large amount of available data, but was difficult for the Middle Jurassic. The empirically determined transformation ratios were compared with transformation ratios based on standard Lawrence Livermore National Labs (LLNL) kinetics as used in Cornford *et al*. (1998) (Fig. 5). As Fig. 5 shows, the Upper Jurassic source rocks plot between the transformation ratios for Type II and Type III using LLNL kinetics, and give a fairly good match for a mixture of Type II and III kerogens. The curve of the upper Draupne Formation with highest Type II kerogen content is most similar to the LLNL Type II curve, while the curve for the Heather Formation consisting of Type III material is nearly identical to the LLNL Type III curve. The transformation ratios obtained by empirical determination, however, seem slightly to overestimate transformation at depths down to 4,000 m TVDss relative to the transformation ratios based on the kinetic model.

The transformation ratios for the Middle Jurassic Vestland Group are also shown in Fig.5, but, as mentioned above, the determination of the ratio was hampered due to the small amount of data available. The Vestland Group curve is similar to the LLNL Type III curve down to 4,400 m, but it is considerably lower below this depth.

Variations in source rock potential

Bulk parameters

The studied dataset from the upper Draupne Formation shows an average measured Hydrogen Index of 267 g HC/kg C_{org}. After restoration, the Hydrogen Index

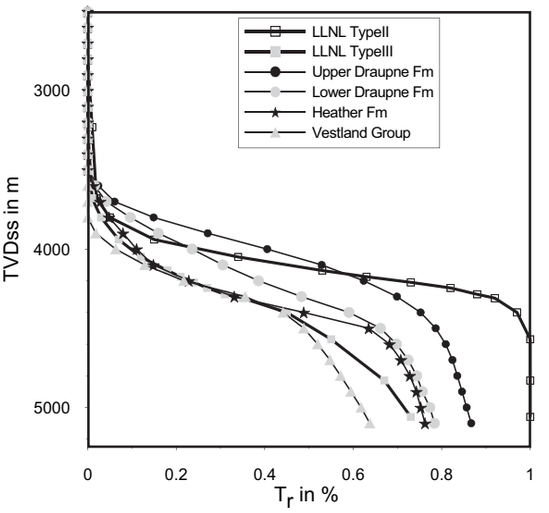

Fig. 5. Comparison of empirically-determined transformation ratios for the upper and lower Draupne Formation, the Heather Formation and the Middle Jurassic Vestland Group, with transformation ratios for Type II and III kerogen based on standard Lawrence Livermore National Lab kinetics (as used in Cornford et *al*., 1998). Ratios are plotted versus depth (not vitrinite reflectance), based on a regional vitrinite reflectance-depth relationship.

shows a bimodal distribution (Fig. 6) with peaks at around 300 and 450 g HC/kg C_{org}. This derives from the fact that only the mature samples are corrected, which form a second peak. The distribution suggests that the upper Draupne Formation contains a mixture of Type II and Type III kerogen with a higher contribution of Type II source material. Average restored TOC is 5.3 wt% and the samples show a TOC range of up to 12 wt%. The lower Draupne Formation shows a considerable lower average restored Hydrogen Index of 234.2 g HC/kg C_{org} and a more unimodal distribution, indicating a greater proportion of terrestrial dominated kerogen of Type III to II (Fig. 6). The average restored TOC is 4.1 wt%. Even lower average restored TOC and Hydrogen Index values of 3.6 wt% and 184.2 g HC/kg C_{org} respectively, are typical for the Heather Formation. The Middle Jurassic Vestland Group is difficult to evaluate and average values for TOC and Hydrogen Index are of little use as no lithological differentiation between coals and non-coaly samples has been made. TOC ranges up to 80 wt%, while restored Hydrogen Indices reach up to 400 g HC/kg C_{org} (Fig. 6).

Gamma-ray log character and vertical changes in HI and TOC

Correlation of the Upper Jurassic section using well logs is difficult in the South Viking Graben. While the basinal sections are thick, are often expanded by mass flow deposits and span a long time interval, the sections on the high are thin and incomplete due to erosion and non-deposition. The upper Draupne Formation is often found to rest directly on the Heather Formation on highs in the area. However, a number of general observations can be made. Thus, a general increase in gamma-ray values up to the top of genetic sequence C2 or the base of sequence D (Fraser *et al*., 2003) in the Middle Volgian can be observed, with gamma-ray API values up to 300 (Fig. 7). This peak appears to be of basinwide extent and is only missing where the section is eroded. Overlying this "hot" interval, which corresponds to the hot shale of Kubala *et al*. (2003), is one unit with slightly lower gamma-ray values and another unit with elevated values on top of the section which is not present everywhere. Kubala *et al*. (2003) made similar observations in the East Shetland Basin and defined a hot shale unit followed by an upper cool shale and an upper hot shale.

The peak of the gamma-ray log coincides with the boundary chosen for the syn- and post-rift sections in this study, for example in wells *15/2-1*, *15/3-3* and *15/9-18* (Fig. 7). In other wells, for example *15/3-1S* and *15/3-5*, this peak occurs slightly earlier or later. The time of this gamma-ray peak coincides roughly with a regressive period in the mid-Volgian (Fig. 2) (Fraser *et al*., 2003).

These observations were used to divide the Upper Jurassic into syn- and post-rift packages, in combination with the Pr/Ph ratio which tends to change from a general upward decrease to a slight increase at the same time (Fig. 7). Kubala *et al*. (2003) used a similar subdivision and grouped their "hot shale" and the overlying units as an "upper facies" and the underlying units as a "lower facies" of the Kimmeridge Clay Equivalent. TOC values generally tend to follow the gamma-ray trend and are overall higher in the upper Draupne Formation. In addition, a general upwards increase of the Hydrogen Index was observed (Fig. 7) as previously described by Dahl and Speers (1985), Huc *et al*. (1985) and Justwan and Dahl (2005). Hydrogen Index values were all maturity corrected; therefore, this trend must be related to the source facies. The topmost section may, however, show a slight decrease in Hydrogen Index, as was also observed by Justwan and Dahl (2005).

The similarity between the East Shetland Basin and the South Viking Graben suggests the rather uniform development of the Kimmeridge Clay Equivalent in

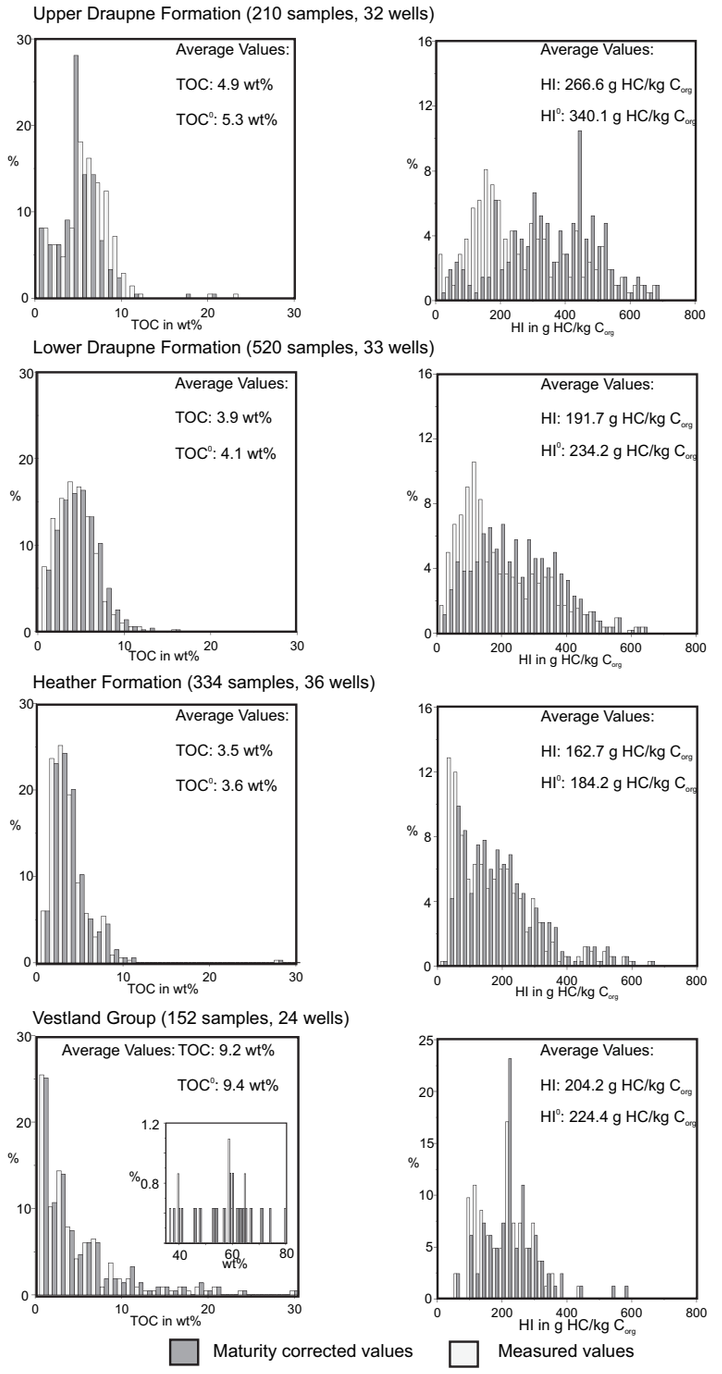

Fig. 6. Histograms for measured and maturity-corrected TOC and Hydrogen Index for the Upper and Middle Jurassic source rock sections. The histograms for the Vestland Group include samples from the Hugin and Sleipner Formations. Hydrogen Indices are much more affected by the maturity correction than TOC values.

the North Sea area, extending south into the Central Graben (*pers. comm.* Iain Scotchman).

Oil and gas potential

The source rock potential of the Upper Jurassic source rock intervals was quantified using the method described by Dahl *et al*. (2004) and Justwan and Dahl (2005). This method is a practical and rapid means to assess the average amount of oil- and gas-producing constituents in a source rock when only Rock-Eval and TOC data are available, as is the case for this study. A cross-plot of maturity-corrected Rock-Eval S2 and TOC was used to determine the amount of inert organic carbon represented by the intercept of

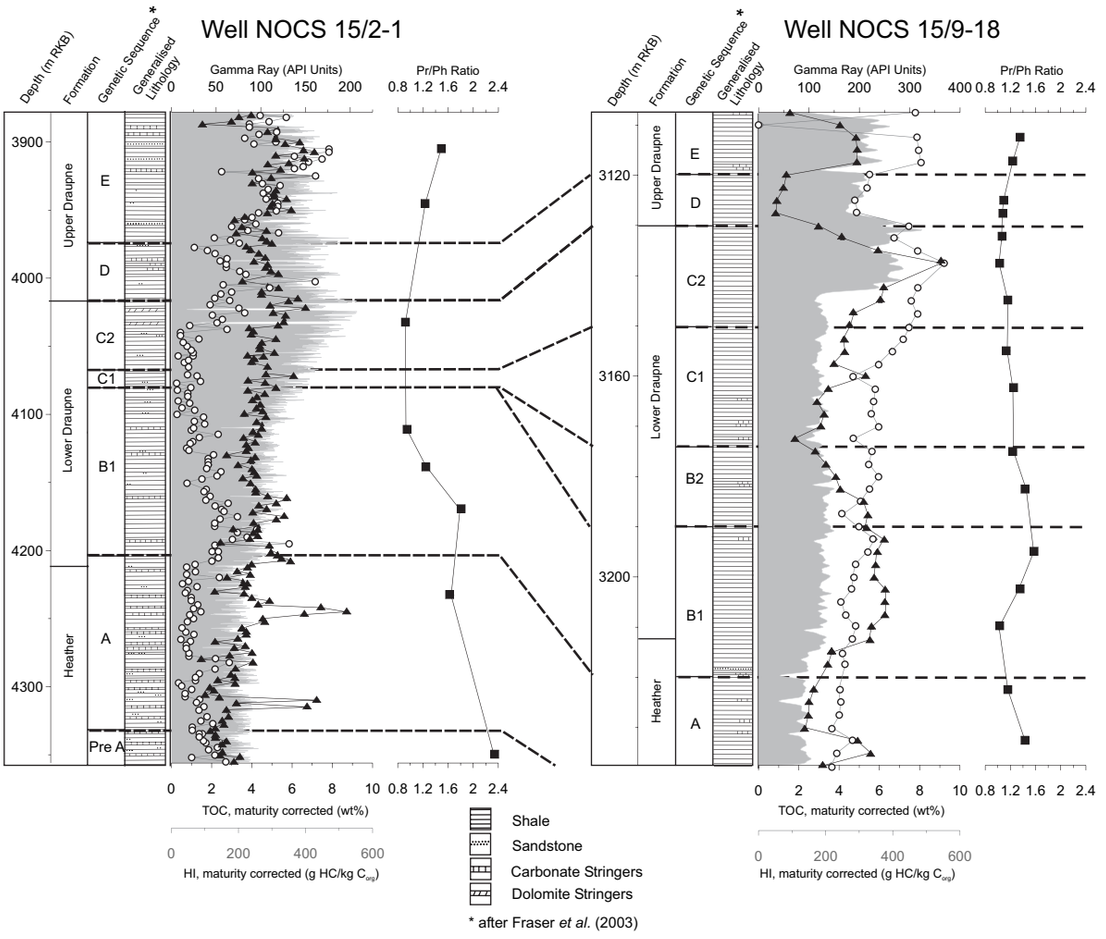

Fig. 7. Gamma-ray log profile, maturity-corrected TOC (black triangles) and Hydrogen Index (open circles) together with Pr/Ph ratio (black squares) for wells *15/2-1* and *15/9-18* (for well locations, see Fig. 1). The gamma-ray peak coincides roughly with the boundary between the upper and lower Draupne Formation. A maturity-independent upward increase of the Hydrogen Index can be observed. Although a general decrease of the Pr/Ph ratio can be observed, the trend changes at the boundary between the upper and lower Draupne Formation from a decrease to a slight increase upwards. This observation and the gamma-ray profile can be used to divide the Draupne Formation.

the regression line with the TOC axis, and to deconvolute the remaining active TOC into oil- and gas-prone fractions. The active TOC represents a mixture of two end-member kerogens with Hydrogen Index values of 675 and 150 g HC/kg C_{org}, respectively. The end-member values have been chosen to fit the dataset. The oil-prone part of the active TOC is referred to as TOCII, while the gas-prone TOC is termed TOCIII. Both are determined for a suite of samples and do not represent individual sample values. Table 1 shows general source rock properties, including TOCII, III and IV (inert TOC) for the Upper Jurassic source rock section in all the wells studied.

The upper Draupne Formation generally shows the highest oil-prone TOCII values with an average of 2.8 wt%, while the lower Draupne contains less oil-prone material with an average 1.75 wt%; the Heather Formation has the lowest oil-prone TOC of 1.05 wt% (Fig. 8). This supports the general observation that the upper Draupne Formation has the highest oil potential. The content of gas-prone organic matter increases slightly from the upper Draupne Formation to the lower Draupne and Heather Formation from 1.11 wt% to 1.29 and 1.27 wt%, respectively. Values for TOCIV between 1.11 and 1.65 wt% are in agreement with those recorded by Barnard *et al*. (1981), indicating that inertinite is a persistent component in the basin. Ramanampisoa *et al*. (1994) observed a constant contribution of approximately 1 wt% inert organic matter in their study of a thin core section of the onshore Kimmeridge Clay in the UK. Absolute values and percentages of TOCII increase upwards, while inert and gas-prone matter show fairly constant absolute values and decreasing proportions upwards (Fig. 8). This suggests that degree of dilution

	Upper Draupne Fm					Lower Draupne Fm					Heather Fm				
	TOC					TOC					TOC				
Well	II	III	IV	n	HI^0	n	II	III	IV	n	HI^0	n	II	III	IV	n	HI^0	n
15/02-1	1.94	0	3.17	54	262	54	0.55	0.46	3.52	74	102.2	77	0	1.6	1.56	54	74.4	55
15/03-1S	3.5	3.23	0.17	10	445.4	12	0.81	2.8	1.1	26	190.2	26	0	2.33	0.98	2	82	4
15/03-2	1.55	1.13	0.92	7	308	7	0.57	2.45	1.38	7	146.4	7	0	1.13	0.9	4	62.7	4
15/03-3	3.49	0.06	2.99	25	353	27	0.77	2.2	2.1	43	116.7	45	0.17	5.56	0.27	5	177.4	5
15/03-5	0.29	0.41	1.2	4	135.1	4	0.29	1.63	1.28	14	135.7	14	0	0.47	0.79	10	35	10
15/05-1	1.76	1.56	0.98	4	276.7	4	3.02	0	4.79	5	282.9	5					275.3	1
15/05-2					424.8	1					200	2	1.41	0.8	2.59	17	209.8	16
15/05-3			no data				0.01	0.7	0.73	15	57.4	15			not present			
15/06-2					505.4	2	4.2	1.05	2.55	3	370.9	3	1.45	1.44	2.11	11	209.3	11
15/06-7			no data				3.48	0	2.09	9	348.8	10	0.32	1.36	1.12	2	167.6	3
15/06-8S	5.57	0	0.59	4	585.4	4			not present				2.25	0.14	1.11	5	419.1	5
15/08-1			no data				2.86	0	2.56	2	365.24	2	1.36	2.42	0.62	5	293.8	5
15/09-2			not present				1.09	2.79	1.92	8	164.9	8			no data			
15/09-3			not present				3.54	3.13	0.13	2	417.5	2			no data			
15/09-11			not present						no data								399	1
15/09-18	1.55	0.66	0.39	8	349.8	9	2.14	1.89	0.78	32	353.4	33	0.78	2.23	0.39	8	245.8	8
15/12-10S			not present						not present				0.23	0.51	0.46	22	183.7	22
15/12-11S			not present				2.19	2.03	0.78	9	358.4	9	0.36	2.92	0.22	14	188.8	15
16/01-2	0.02	0.18	0.4	2	106.6	3	1.09	0	1.1	56	278.2	58	0.67	0.76	1.27	14	187.1	15
16/01-3			not present				0.49	1.39	0.12	2	175.8	2					310.1	2
16/07-2			not present				1.16	0.54	1.3	28	254.3	30			not present			
16/10-2			not present				6.18	0	1.11	5	590.4	5			not present			
16/10-3	3.28	0.63	0.59	5	456.1	5			not present						not present			
16/10-4	5.61	1.87	0.51	3	516.4	3			not present						not present			
16/11-2			not present				3.07	0	3.42	2	409	2	4.36	0.18	1.36	2	498.8	2
24/06-1			not present				1.38	0	2.47	3	280.8	3	1.04	0	1.86	17	265.6	17
24/09-1	3.16	1.86	0.98	23	337.6	23	2.15	2.74	0.61	34	341.8	34			not penetrated			
24/12-1R	1.77	2.9	2.03	4	228.2	5	0.83	1.68	2.69	9	157.1	9					176	2
25/01-10	1.66	3.68	1.86	2	414.3	3	0	0.8	0.36	8	74.6	8	0.55	1.13	1.14	32	120.9	32
25/02-12			no data						no data				0.13	0.66	1.11	5	84.6	7
25/02-14			no data				2.9	0	3.63	3	313.6	3	1.15	0.11	0.34	5	402.6	6
25/03-1					389.4	3					399.9	1	1.38	2.24	1.58	5	214.9	5
25/04-1			not present				0	3.96	1.59	2	118.3	3			no data			
25/05-2	4.04	1.73	0.83	5	460.7	5	2.39	1.59	3.32	7	252.1	7	2.34	0	3.54	4	288.6	4
25/05-3			not present						not present				1.21	0.77	1.12	2	278.1	2
25/06-1	5.21	0	2.64	5	492.3	5			not present				2.71	0	2.01	8	308.9	8
25/06-2	5.16	0	1.43	2	585.6	2					619	1					487.6	2
25/07-2	3.15	1.77	2.08	5	337	5	0.84	1.52	0.91	71	241.8	73	0.48	0.66	1.31	22	174.6	26
25/08-5S					72.7	1			no data								43	1
25/08 - 7			not present						no data				2.9	1.77	0.13	3	443.8	3
25/09 - 1					636.8	1			not present				1.36	0.1	0.74	6	297.4	5
25/10-6S			no data								127	1					120.9	2
25/10-8A	1.47	0	1.09	8	401.1	8	0.59	0.71	0.3	10	320	10			not penetrated			
25/11-15	0.53	0.72	0.55	3	168.6	3			not present						not present			
25/11-17					34.5	1			not present						not present			
26/04-1	4.88	0.31	1.41	7	508.6	7					345.5	3	0.25	1.53	0.32	5	173	5
30/12-1					433	1	2.18	1.28	0.84	4	322.5	4	0.56	2.76	0.18	2	223	2

Table 1. Maturity-corrected values for oil- and gas-prone and inert organic matter and average values of the Hydrogen Index for the upper and lower Draupne and Heather Formations for all wells used in the source rock mapping process (for well locations, see Fig. 1). Hydrogen Index (HI) in g HC/kg C_{org}, all TOC values in wt%.

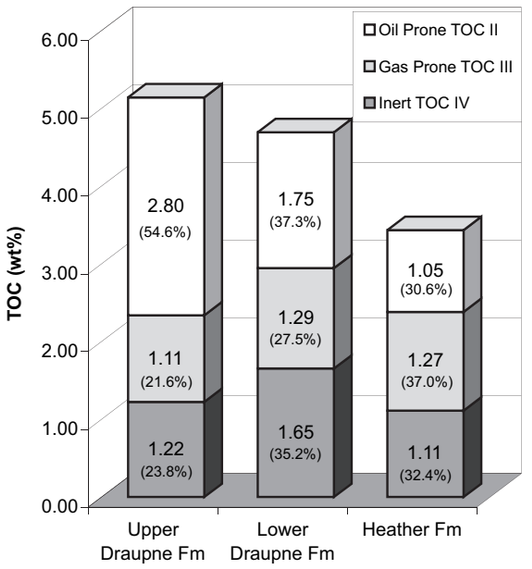

Fig. 8. Average distribution of oil- and gas-prone and inert organic matter in the Upper Jurassic source intervals in wt% (in brackets: proportion in percent of total TOC). Increasing amounts of marine organic matter from the Heather to the upper Draupne Formation are added to near constant values of inert organic matter. Terrestrial, gas-prone organic matter is least abundant in the upper Draupne Formation.

by gas-prone and inert material decreases upwards, and increased input and/or preservation of oil-prone material dominates the upper Draupne Formation.

In order to evaluate the regional variations in source potential and to investigate the effect of dilution by mass transport from surrounding highs on the distribution of organofacies and source potential, maps of the oil- and gas-prone TOC as well as the inert TOC were generated from well data by convergent trend gridding in *IRAP*. Approximate outlines of mass flow sands after Fraser *et al*. (2003) are added for visual comparison.

Heather Formation

The least oil-prone Upper Jurassic unit in the South Viking Graben is the Heather Formation. Oil-prone TOC values rarely exceed 2 wt% and are below 1 wt% in Blocks 24/9, 24/12 and 15/3. Interestingly, TOCII values increase towards the High in the east (Fig. 9g). This could be interpreted as an effect either of enhanced productivity or of reduced siliciclastic dilution. Maximum values are encountered in Blocks 25/5, 25/8, 25/6 and in the Ling Graben. The values for gas-prone matter decrease towards the east and high values are only encountered in the depocentres in the west where sediments were concentrated (Fig. 9h). Although the influence of mass flows is less pronounced in the Heather Formation (Fraser *et al*., 2003), regions with elevated values for TOCIII (Fig. 9h) coincide with areas which received mass flows. High values of TOCIII on the western side of the study area appear to be related to transport of gas-prone and reworked material by mass flows.

High values of TOCIV on the northern edge of the Utsira High may be explained in terms of reworked and gas-prone material being swept from the nearby high, while elevated TOCIV values in Block 15/5 could be related to mass flow processes (Fig. 9i).

Lower Draupne Formation

The thick lower Draupne Formation also shows generally low oil-prone TOC values, particularly in the currently mature graben area in Blocks 15/3, 24/12 and 24/9 (Fig. 9d). The Sleipner Terrace and the Ling Depression show the highest values, but are currently immature. Similar to the Heather Formation, the lower Draupne Formation also shows an eastward decrease in TOCIII (Fig. 9e). The main contribution of gas-prone material appears to originate from the west, from the East Shetland Platform. Exceptionally high values of TOCIII are encountered in Blocks 24/12, 15/3 and 15/2, areas which received mass flows from the East Shetland Platform and the Utsira High during deposition of the lower Draupne Formation (Fig. 9d). The correlation of highly gas-prone areas with mass flows (Fig. 9d) indicates that gas-prone organic matter has been transported from the East Shetland Platform via these mass flows.

Another highly gas-prone area is the northern edge of the Utsira High in Block 25/4. This area also shows elevated amounts of inert organic matter, probably derived from the nearby Utsira High. Remarkably high values of TOCIV are also encountered in Blocks 15/8, 15/5 and 15/2 where mass flows from the East Shetland Platform shed reworked organic matter to the east (Fig. 9f).

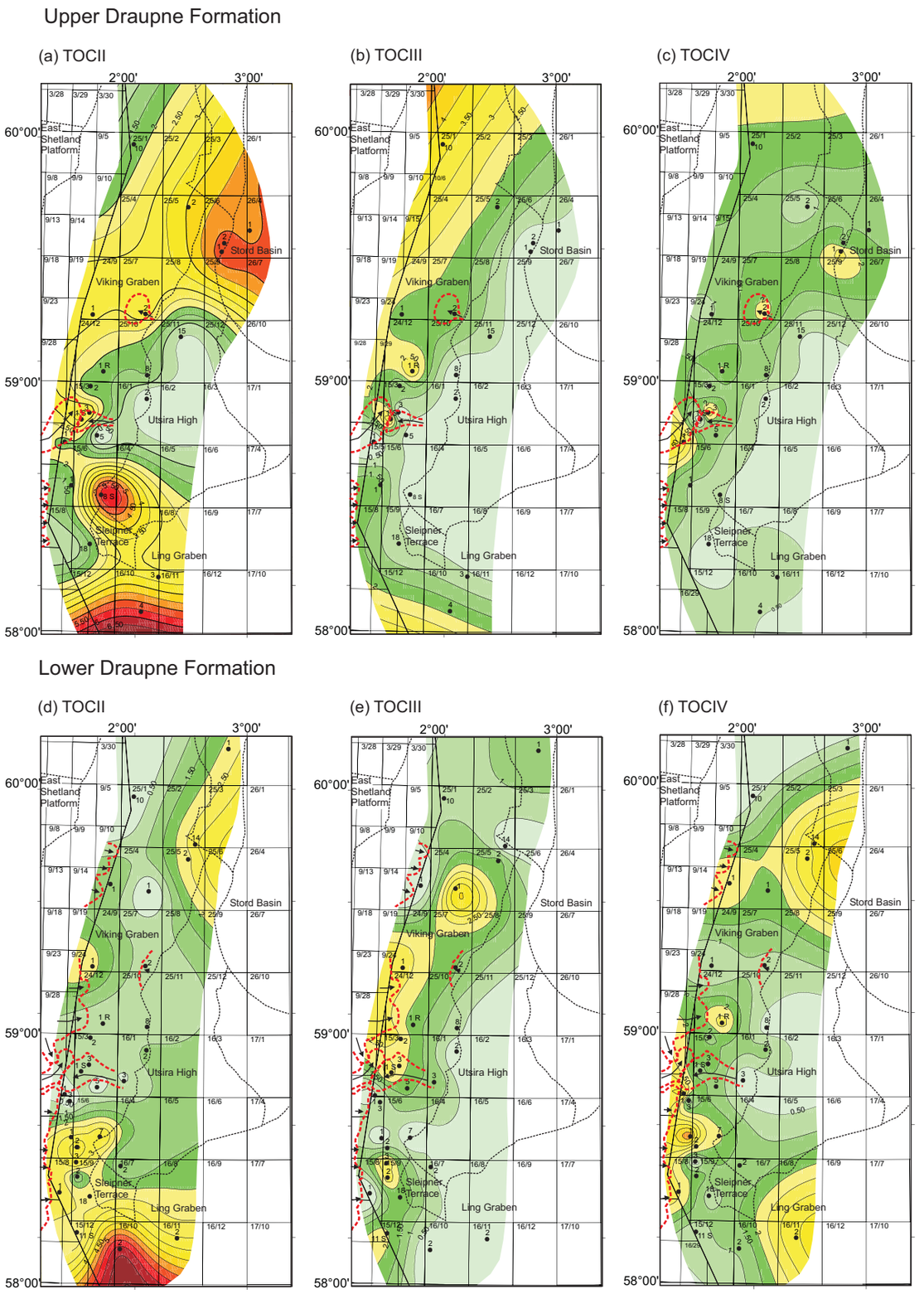

Fig. 9. Quantitative source rock potential maps (maturity-corrected) of the Upper Jurassic section in the South Viking Graben.
(a-c) oil-prone, gas-prone and inert organic matter for the upper Draupne Formation.
(d-f) oil-prone, gas-prone and inert organic matter for the lower Draupne Formation.
(g-i) (facing page) oil-prone, gas-prone and inert organic matter for the Heather Formation.
Approximate maximum extent of mass flow sands after Fraser *et al.* (2003).

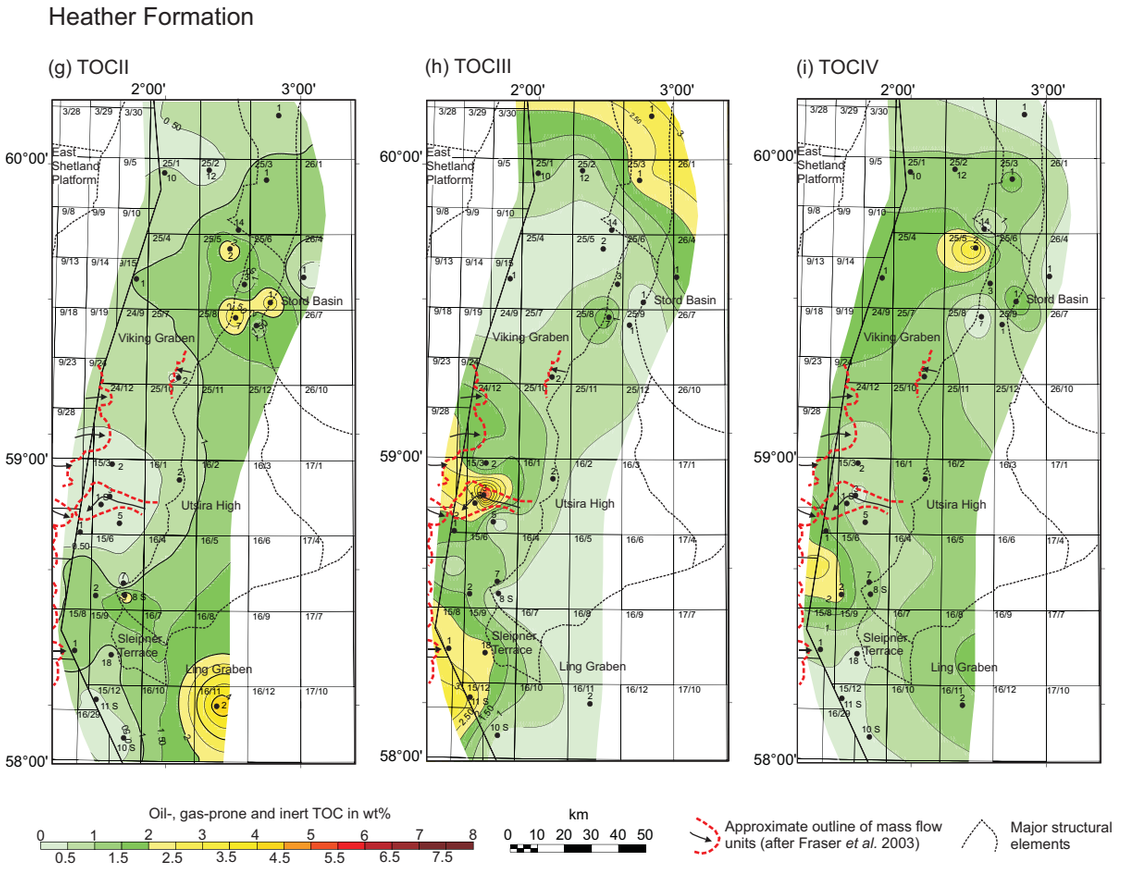

The maps in Fig. 9 clearly show the influence of gas-prone and inert organic matter transported by mass flows and their dilution effect. In the fairly narrow South Viking Graben, gas-prone as well as reworked material may have reached the deepest part of the graben from both flanks. This led to a complex mixing of oil- and gas-prone organic matter.

Upper Draupne Formation

The maps for the upper Draupne Formation illustrate the significantly different organic facies within this section. Oil-prone organic matter reaches 3.5 wt % in most of the study area (Fig. 9a). Maxima occur on the western flank of the Stord Basin in Blocks 25/6 and 26/4, on the southern edge of the Utsira High in Block 15/6 and in the Ling Depression, areas which are all currently immature. Minimum values are encountered on the Utsira High in Blocks 16/1 and 25/11. A further zone of low oil potential is located in Blocks 24/12, 15/3 and 15/5, where mass flows of the Brae trend remained active (Fraser *et al*., 2003).

The amount of gas-prone organic matter is generally lower than of oil-prone material and again shows an eastward decrease towards the Utsira High (Fig. 9b). In contrast to the lower Draupne Formation, mass flows are scarce and are only present in the lowermost section of the post-rift upper Draupne Formation (Fraser *et al*., 2003). The input of gas-prone and inert organic matter resulting from mass flows is therefore greatly reduced.

Another factor that may contribute to small amounts of gas-prone material is that during late phase rifting and subsequent quiescence, the greater depth and the elongated basin shape favoured water stratification and algal productivity, while the uplift of the shoulders restricted terrestrial input (Huc, 1990). Wignall and Ruffell (1990) related the reduced terrestrial input in the Wessex Basin to climatic change towards arid conditions from the Early Volgian onwards. This may also be applicable to the study area. Elevated values for TOCIII are shown in Block 25/1 and can be interpreted as run-off from the East Shetland Platform, as this area shows an additional regional low in oil-prone organic matter content. Inert, reworked organic matter (Fig. 9c) ranges from 0.5 to around 2 wt% in the graben area in the upper Draupne Formation. The maximum values encountered in Blocks 15/3 and 15/2 as well as Block 25/7 appear to be associated with mass flows originating from the East Shetland Platform and the Utsira High (Fig. 9c).

Another area showing elevated values of TOCIV, which can be related to transport of reworked organic matter from the nearby Utsira High, is located in Block 25/6 on the western flank of the Stord Basin.

	Depth		Rock-Eval		GC Ratios					GCMS Ratios							
Well	m RKB	Formation	TOC^0	HI^0	A	B	C	D	E	F	G	H	I	J	K	L	M
15/3-3	4065	Upper Draupne	19.64	246.5	1.27	0.55	0.49	0.72	1.17	0.22	1.43	0.58	0.34	0.42	0.96	1.26	1.2
15/3-3	4070	Upper Draupne	10.43	305.2	1.31	0.54	0.47	0.76	1.02	0.25	2.29	0.58	0.1	0.37	0.91	1.31	1.18
15/3-3	4090	Upper Draupne	8.15	303.3	1.27	0.53	0.49	0.76	1.02	0.24	2.76	0.59	0.08	0.35	1.05	1.2	1.15
15/3-3	4095	Upper Draupne	5.62	347.2	1.17	0.59	0.55	0.72	0.98	0.24	3.33	0.6	0.08	0.36	1	1.31	1.16
25/7-2	4058	Upper Draupne	5.51	299.8	1.21	0.4	0.41	0.86	0.99	0.24	6.31	0.56	0.13	0.42	1.11	1.4	1.16
25/7-2	4070	Upper Draupne	8.17	344.6	0.97	0.35	0.42	0.83	1.02	0.3	5.83	0.57	0.14	0.39	1.06	1.51	1.13
15/9-18	3117.5	Upper Draupne	4.88	484	1.23	0.57	0.56	0.77	0.82	0.27	0.49	0.6	0.17	0.61	0.82	1.21	1.47
15/9-18	3127.5	Upper Draupne	0.87	296.6	1.07	0.67	0.61	0.66	0.82	0.29	0.55	0.54	0.17	0.96	0.83	1.21	1.44
15/3-3	4175	Lower Draupne	9.94	232.6	1.46	0.36	0.36	0.92	1.05	0.09	3.68	0.6	0.09	0.48	1.63	1.05	1.01
15/3-3	4325	Lower Draupne	5.14	125.8	1.43	0.4	0.34	0.79	1.05	0.07	2.81	0.59	0.06	0.43	1.48	1.36	1
15/3-3	4416	Lower Draupne	5.71	164	1.87	0.64	0.43	0.78	1.04	0.08	2	0.6	0.12	0.71	2	1.18	0.88
15/3-5	3840	Lower Draupne	4.04	195.7	1.43	0.66	0.64	0.73	1.12	0.12	1	0.59	0.13	0.41	1.27	1.1	0.95
16/7-2	2584	Lower Draupne	3.45	378	1.68	0.96	0.79	0.88	1.15	0.04	0.33	0.46	0.19	0.49	0.83	0.57	0.86
25/1-10	4305	Lower Draupne	1.14	72.9	1.94	0.36	0.24	0.86	1.01	0.13	1	0.53	0.15	0.9	1.67	1.12	1.17
25/7-2	4118	Lower Draupne	5.49	155.1	1.46	0.54	0.53	0.91	1	0.16	5.06	0.59	0.1	0.7	1.33	1.52	1.07
15/9-18	3182.5	Lower Draupne	4.05	329.4	1.45	0.78	0.6	0.68	0.94	0.12	0.4	0.55	0.21	0.67	2.16	1.17	1.24
25/5-2	3150	Heather	3.71	101.1	2.83	1.4	0.35	0.66	1.3	0.35	0.18	0.6	0.26	0.79	1.6	0.96	0.74
25/5-2	3160	Heather	6.23	465.3	2.04	0.89	0.52	0.75	1.25	0.04	0.45	0.6	0.18	0.64	1.64	1	1.22
25/1-10	4320	Heather	1.04	61.2	1.86	0.39	0.27	0.91	1.06	0.07	1.25	0.61	0.14	0.94	1	1.3	1.42
25/1-10	4330	Heather	1.21	69.3	2.19	0.42	0.26	0.89	1.04	0.06	1.6	0.54	0.15	0.86	7	1.44	1.23
25/1-10	4340	Heather	0.95	50	2.11	0.48	0.32	0.88	1.08	0.07	1.04	0.6	0.13	1.04	1.4	1.21	1.13
25/1-10	4380	Heather	2.67	170.1	1.87	0.43	0.25	0.79	1.38	0.07	1.02	0.58	0.14	0.89	1.6	1.12	1.19
25/7-2	4400	Heather	4.67	114.5	1.73	0.89	0.73	0.91	1.03	0.16	1.77	0.64	0.24	0.95	2.25	1.57	1.3
15/9-18	3232.5	Heather	4.87	281.5	1.43	0.61	0.49	0.64	0.95	0.17	0.68	0.58	0.18	0.63	1.27	1.48	1.5
15/9-18	3280	Hugin	58.65	121.6	5.86	8.79	1.11	0.24	0.93	0.4	0.05	0.58	0.35	1.39	8.18	0.13	0.24
16/7-2	2674	Hugin	9.71	181.7	2.4	0.75	0.54	0.91	0.94	0.65	0.24	0.42	0.32	0.56	1	1.25	0.81
25/7-2	4433	Hugin	1.54	83	1.56	0.82	0.66	0.93	1.14	0.1	1.24	0.6	0.13	0.95	1	1.13	1.13
15/3-5	3940	Sleipner	2.82	116.3	3.69	0.87	0.22	0.48	1.19	0.02	0.21	0.6	0.12	0.67	2.9	0.67	0.36
15/9-18	3430	Sleipner	4.11	217	2.27	0.99	0.41	0.52	1.04	0.11	0.08	0.51	0.34	0.85	1.36	0.89	0.79
15/9-18	3560	Sleipner	1.81	131.5	1.91	0.7	0.41	0.49	0.85	0.16	0.23	0.51	0.28	0.88	1.57	0.99	0.95

Table 2. Maturity-corrected TOC and Hydrogen Indices, GC and GCMS ratios for selected source rock samples from the upper and lower Draupne Formation as well as the Heather, Hugin and Sleipner Formations. For descriptions of the parameters, see Table 3.

A	Pristane/Phytane ratio	Brooks *et al*. (1969); Didyk *et al*. (1978)
B	Pristane/n-C_{17}	-
C	Phytane/n-C_{18}	-
D	Waxiness: n-C_{17}/(n-C_{17}+n-C_{27})	-
E	Carbon Preference Index (CPI)	Bray and Evans (1961)
F	BNH%: 17α(H),21β(H) -28,30-bisnorhopane versus 17α(H),21β(H)-28,30-bisnorhopane + C_{30} hopane	Isaksen *et al*. (1998)
G	Ts/Tm	Seifert and Moldowan (1985)
H	22S: Ratio of 17α(H),21β(H), 22(S) bishomohopane versus 17α(H),21β(H),22(S) + (R) bishomohopanes	Seifert and Moldowan (1986)
I	30βα/30αβ: ratio of C_{30} moretane versus C_{30} hopane	Isaksen and Bohacs (1995)
J	C_{29} versus C_{30} hopanes	after Peters and Moldowan (1993)
K	C_{34}/C_{35} : Ratio of C_{34} versus C_{35} homohopanes	after Peters and Moldowan (1991)
L	Ratio of C_{27}-C_{29} diasteranes versus C_{27}-C_{29} regular steranes	after Peters and Moldowan (1993)
M	C_{27}/C_{29}: Ratio of C_{27} ββ(R+S) steranes versus C_{29} ββ(R+S) regular steranes, measured in m/z 218	Huang and Meinschein (1979)

Table 3. Description of selected facies-indicating GC and GCMS parameters given in Table 2.

The distribution of oil- and gas-prone organic matter does not follow the commonly observed pattern whereby the highest potential is in the deepest parts of the graben and there is increasing terrestrial dominance towards the highs (Fisher and Miles, 1983; Thomas *et al*., 1985). Rather, the deeper graben areas, acting as sediment traps, show the highest content of terrestrial material.

Molecular source facies and isotopic characteristics

The molecular and carbon isotopic characteristics of the Upper and Middle Jurassic source rocks were investigated to support the source potential mapping and to gain a better understanding of the regional and stratigraphic trends in geochemical properties. The carbon isotopic composition of the saturate and aromatic fraction of source rock extracts reflects variations in kerogen type and source maturity, but might also be affected by factors such as temporal variations in carbon cycling or local changes in paleoproductivity (Tyson, 2004). The distribution of triterpanes and steranes analysed by GCMS also gives valuable information on source rock depositional environment and development of the Jurassic source rock system. Biomarker ratios for selected samples are listed in Table 2.

Geochemical characteristics of Middle Jurassic source rocks

Molecular and isotopic characteristics of Middle Jurassic source rocks show a great deal of variation as the samples represent different lithofacies ranging from mudrocks to coaly shales and coals. Middle Jurassic source rocks in the Hugin and Sleipner Formation are isotopically heaviest with $\delta^{13}C$ values ranging from -24 to -28 ‰PDB for saturate and aromatic fractions (Fig. 10). Coaly samples show the heaviest ratio values while the shaly and sandy samples are generally lighter. This can be interpreted in terms of kerogen type (Cooper *et al*., 1993) as Type III facies for the coaly samples and a higher Type II contribution for the shaly samples.

The extracts from the Middle Jurassic section are dominated by higher molecular weight compounds in the range of *n*-C_{23} to *n*-C_{30} (Fig. 11); the Middle Jurassic source rocks therefore show in general a low *n*-C_{17}/(*n*-C_{17} + *n*-C_{27}) ratio. The presence of these high molecular weight *n*-alkanes in the Hugin and Sleipner Formation can be attributed to terrestrial plant input (c.f. Tissot and Welte, 1984), while the short chain *n*-alkanes are reported to be constituents of algae (Gelpi *et al*., 1970). The dominance of high molecular weight compounds is more pronounced in the Sleipner Formation and the coaly samples, while the shales of the Hugin Formation show a higher proportion of short chain compounds.

The distribution of C_{30} 17β(H),21α(H)-moretane and the corresponding C_{30} 17α(H),21β(H)-hopane also shows high variability. Middle Jurassic samples commonly exhibit the highest moretane contents, indicating the highest terrestrial contribution to the kerogen (Isaksen and Bohacs, 1995) (Fig. 12d). The ratio of rearranged (dia-) steranes to regular steranes also differs in the various sections. Middle Jurassic samples show values approaching unity, while overlying sections show values above unity. The distribution of C_{27} to C_{29} regular steranes was

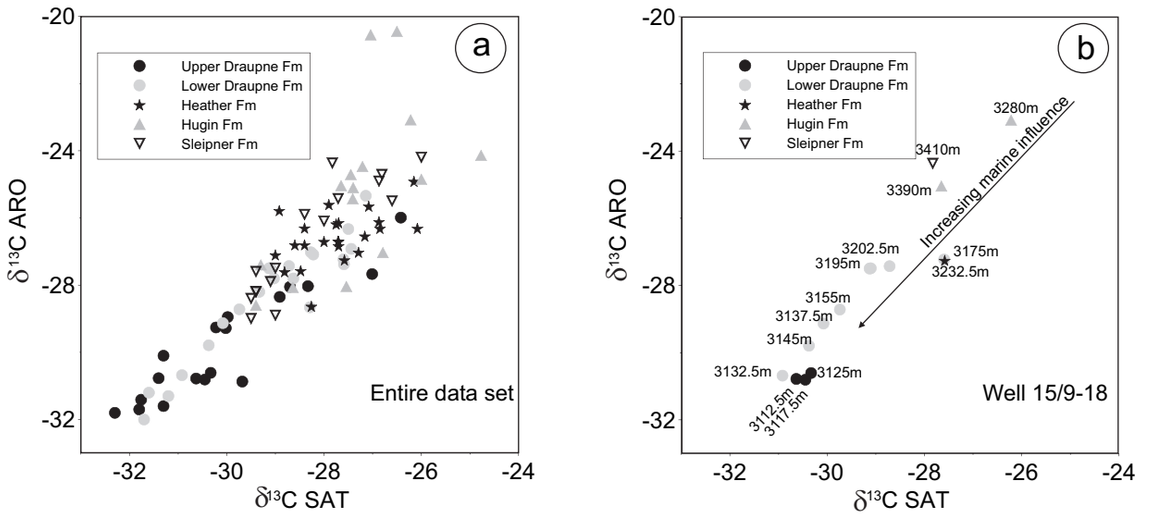

Fig. 10. Stable carbon isotopic composition of aromatic and saturate fraction of source rock extracts. (a) Entire data set; (b) well *15/9-18*, displaying a trend of progressively lighter isotopic compositions from the Middle Jurassic upwards.

determined in the m/z 218 fragmentograms. According to Huang and Meinschein (1979), the dominant source of C_{27} sterols is zooplankton while C_{29} sterols occur mainly in higher plants. It has been found that the ratio of C_{27} versus C_{29} regular steranes increases on average upwards from the Sleipner to the upper Draupne Formation, suggesting an increase in marine, algal influence. Coaly shales and coals show ratio values as low as 0.2 while the ratio in shaly samples can reach 1.1 (Table 2). In general however, the Middle Jurassic extracts show a dominance by C_{29} steranes, indicating a higher input of terrestrial material.

The distribution of acyclic isoprenoids can be used to distinguish the source intervals. Pr/Ph ratios range from *ca* 1.5 for shaly samples in the Hugin Formation to over 6 for coals and coaly shales (Fig. 12c). The Pr/Ph ratio is considered to indicate the degree of oxygenation in the depositional environment (Brooks *et al*., 1969; Didyk *et al*., 1978), although its significance as an indicator of palaeoenvironmental conditions is still debated (Brassell *et al*., 1987; ten Haven *et al*., 1987). High values of the Pr/Ph ratio for Middle Jurassic samples are consistent with the fact that the coaly shales and coals were deposited in an oxygenated fluvio-deltaic environment with a high terrestrial OM input.

Geochemical characteristics of the Heather Formation

The samples of the Upper Jurassic Heather Formation are isotopically slightly lighter than the Middle Jurassic samples with $\delta^{13}C$ for saturate fractions ranging from -26.5 to -28.5 ‰, and for aromatic fractions from -25 to -28.5 ‰PDB (Fig. 10). This can be interpreted using the approach of Cooper *et al*. (1993) in terms of an increased Type II contribution relative to the Middle Jurassic samples. The samples of the Heather Formation often show a bimodal *n*-alkane distribution with maxima from *n*-C_{14} to *n*-C_{18} and *n*-C_{21} to *n*-C_{29} and an odd-over-even carbon number dominance (Fig. 11). Similar to the Middle Jurassic samples, the Heather Formation samples exhibit a high C_{30} moretane content relative to C_{30} hopane (Fig. 12d). The ratio of C_{29} hopane to C_{30} hopane is similar to that in the Middle Jurassic samples and distinctively higher than that in the Draupne Formation samples. C_{34} homohopanes dominate over the C_{35} homologues in the Heather Formation (Fig. 12b), indicating oxidising conditions (Peters and Moldowan, 1993). The Pr/Ph ratio varies significantly between 1.16 and 3.29; its average (1.98) is lower than the average for the Middle Jurassic (Fig.12c), indicating more reducing conditions in the Heather Formation.

Geochemical characteristics of the Draupne Formation

The molecular and isotopic characteristics of the syn- and post-rift sections of the Draupne Formation are very similar. However, certain parameters, such as the Pr/Ph ratio, carbon isotopic composition and the content of 17α(H),21β(H)-28,30-bisnorhopane, may distinguish the syn- and postrift facies.

The samples derived from the upper Draupne Formation are on average isotopically lighter compared to those from the lower Draupne Formation, although there is a large variation in the analysed data (Fig. 10). The bulk of the upper Draupne data shows $\delta^{13}C$ saturate values from -29.5 to 32 ‰PDB and aromatic values between -28.5 and -32 ‰, indicating a relatively high algal contribution to the kerogen

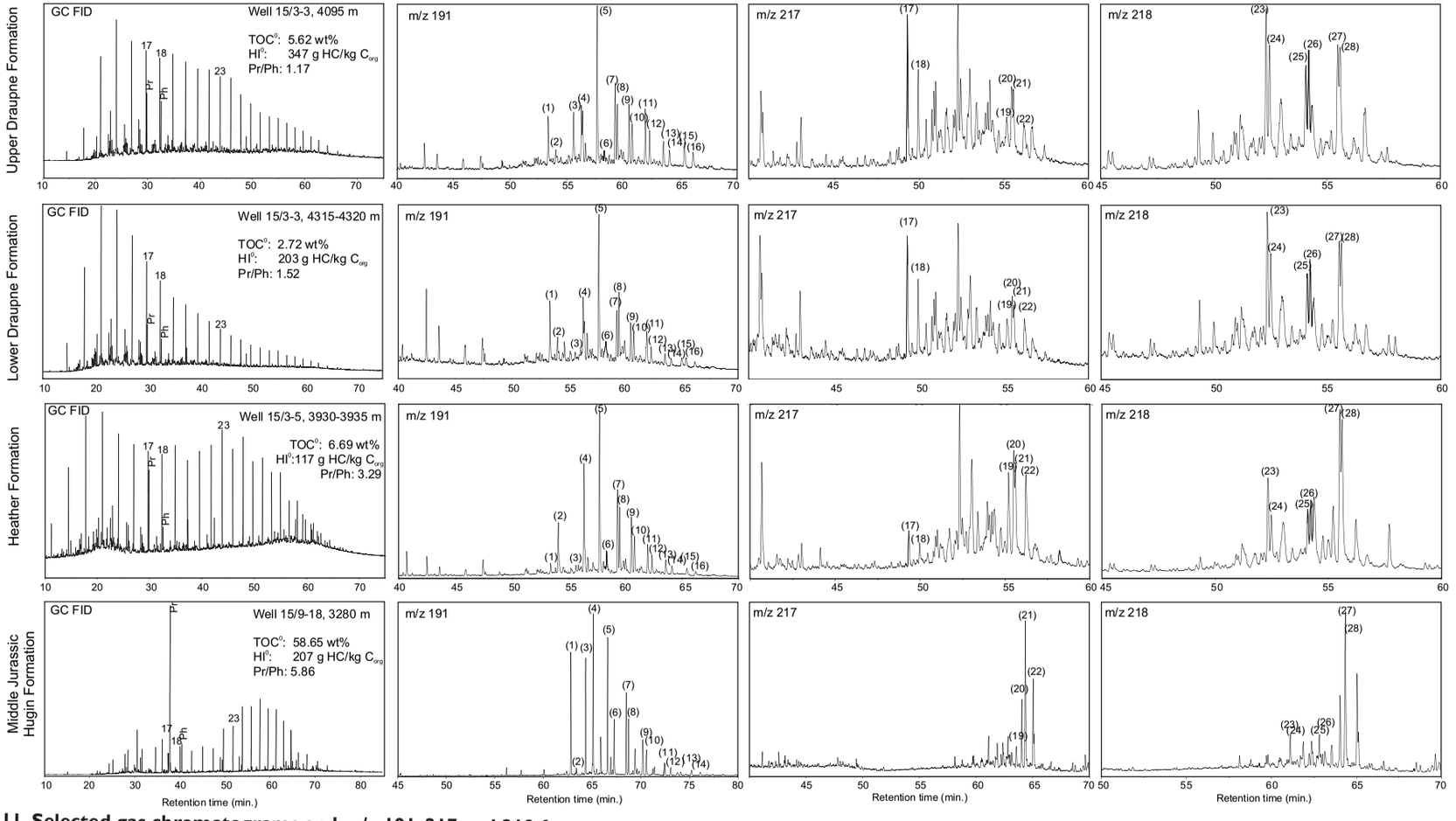

Fig. 11. Selected gas chromatograms and m/z 191, 217 and 218 fragmentograms for the upper and lower Draupne, Heather and Hugin Formations. Compound identification: *n*-alkanes are marked with their carbon number, Pr = Pristane, Ph = Phytane; (1) C_{27} 18α(H)-22,29,30-trisnorneohopane (Ts), (2) C_{27} 17α(H)-22,29,30-trisnorhopane (Tm), (3) C_{28} 17α(H),21β(H)-28,30-bisnorhopane (BNH), (4) C_{29} 17α(H),21β(H)-30-norhopane (29$\alpha\beta$), (5) C_{30} 17α(H),21β(H)-hopane (30$\alpha\beta$), (6) C_{30} 17β(H),21α(H)-hopane (30$\beta\alpha$), (7)-(16) C_{31} to C_{35} 17α(H),21β(H),22(S)+(R) homohopanes, (17) C_{27} 13β(H),17α(H),20(S)-cholestane, (18) C_{27} 13β(H),17α(H),20(R)-cholestane, (19) C_{29} 24-ethyl-5α(H),14α(H),17α(H),20(S)-cholestane, (20) C_{29} 24-ethyl-5α(H),14β(H),17β(H),20(R)-cholestane, (21) C_{29} 24-ethyl-5α(H),14β(H),17β(H),20(S)-cholestane, (22) 24-ethyl-C_{29} 5α(H),14α(H),17α(H),20(R)-cholestane, (23) C_{27} 5α(H),14β(H),17β(H),20(R)-cholestane, (24) C_{27} 5α(H),14β(H),17β(H),20(S)-cholestane, (25) C_{28} 24-methyl-5α(H),14β(H),17β(H),20(R)-cholestane, (26) C_{28} 24-methyl-5α(H),14β(H),17β(H),20(S)-cholestane, (27) C_{29} 24-ethyl-5α(H),14β (H),17β(H),20(R)-cholestane, (28) C_{29} 24-ethyl-5α(H),14β (H),17β(H),20(S)-cholestane.

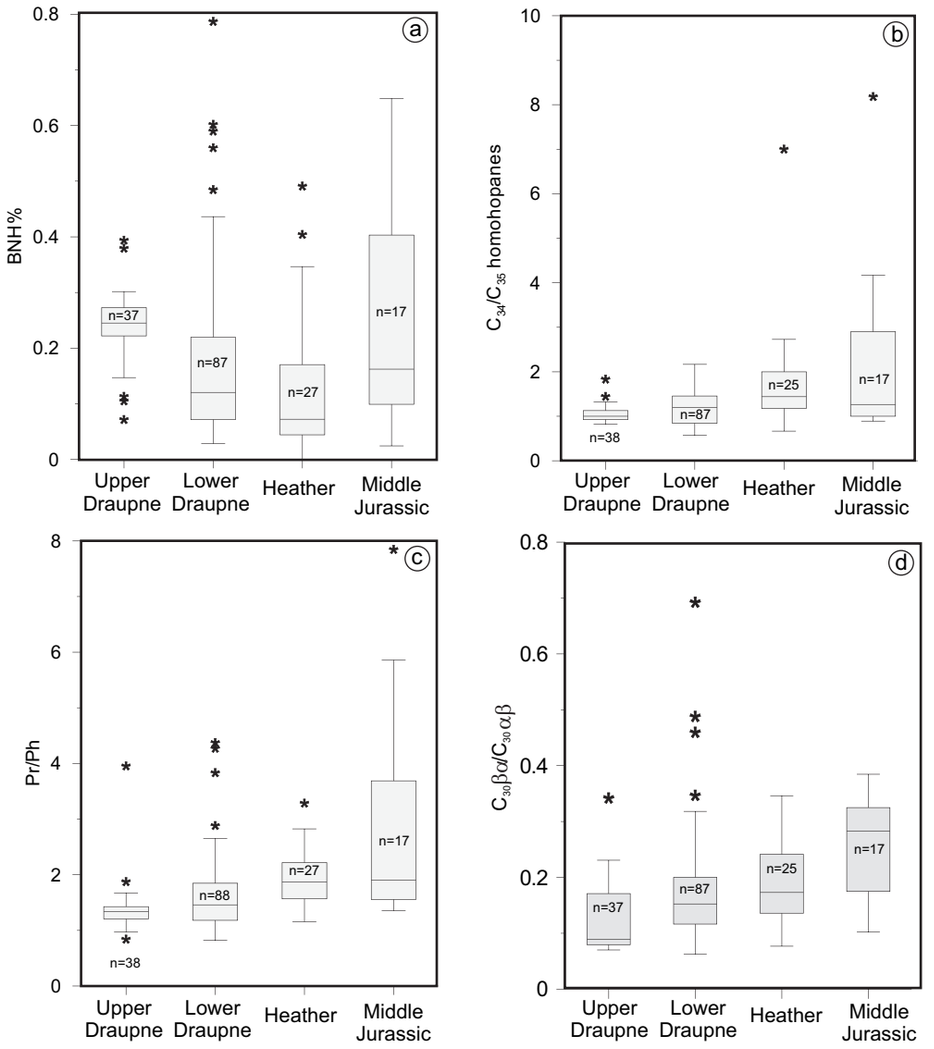

Fig. 12. "Box-and-whisker" plots for selected biomarker parameters:
(a) BNH%: 17α(H),21β(H)-28,30-bisnorhopane vs. 17α(H),21β(H)-28,30-bisnorhopane + C_{30} hopane;
(b) Ratio of C_{34} to C_{35} homohopanes;
(c) Pristane/Phytane ratio; (d) Ratio of C_{30} moretane to C_{30} hopane.
Second and third quartiles are displayed by the box, while the median value is indicated by the line across the box. Outliers shown as * represent values 1.5 times the interquartile range below or above the central 50% of the distribution. The changes in specific wells are more pronounced as the overall statistical distribution shows.

(Cooper *et al*., 1993). Similar values were observed by Kubala *et al*. (2003) for the "upper facies" in the East Shetland Basin, while Thomas *et al*. (1985) reported values between -26.5 and -31.5 ‰ for the Kimmeridge Clay. The bulk of the lower Draupne Formation samples had $\delta^{13}C$ ratios of -27.5 to -30.5 ‰ for the saturate fraction and -26 to -31 ‰ for the aromatic fraction, and can therefore be assigned to a mixture of Type II and III kerogens. The large variation in the lower Draupne Formation relative to the upper Draupne Formation (Fig. 10a) is indicative of the more uniform organic facies of the latter unit. Fig. 10a shows the general distribution of carbon isotope ratios of rock extracts in the area, while Fig. 10b highlights the upward trend towards lighter isotopic compositions for the Jurassic section in well *15/9-18*. These samples are all currently immature and show the same upwards trend towards lighter isotopic compositions as the entire data set, suggesting that this trend is facies related.

The gas chromatograms of the saturate fraction are dominated by compounds ranging from *n*-C_{15} to *n*-C_{17} for both the upper and the lower Draupne Formations (Fig. 11). This is interpreted to indicate an input of algal organic matter (Tissot and Welte, 1984). The CPI values point to differences between

the source rock intervals, with the upper Draupne Formation showing the lowest values. Ratios of C_{34} to C_{35} homohopanes close to unity for the upper Draupne Formation indicate anoxic depositional conditions (Peters and Moldowan, 1991). The dominance of C_{34} homohopanes over C_{35} homohopanes decreases from the Middle Jurassic towards the Upper Jurassic supporting the trend of decreasing degree of oxygenation upwards observed by Justwan and Dahl (2005). The upper Draupne Formation samples show a clear predominance of C_{30} hopanes relative to C_{29} hopanes (Fig. 11), while the distribution of these compounds varies greatly in the lower Draupne Formation, but is higher with ratios between 0.35 and 0.85. This can be interpreted in terms of facies variability indicating a more uniform facies for the upper Draupne. Also, the distributions of C_{30} 17β(H),21α(H)-moretane and the corresponding C_{30} 17α(H),21β(H)-hopane show large variability in the Draupne Formation (Fig. 12d). The uniformly low amounts of moretane in the upper Draupne Formation can be attributed to a small amount of terrestrial organic matter in the kerogen, while the large variation in the lower Draupne Formation signifies a mixed input.

The analysed Upper and Middle Jurassic source rock samples generally contain small amounts of tricyclic terpanes relative to pentacyclic terpanes. The Draupne Formation however often exhibits a high abundance of C_{19} relative to C_{21} tricyclics with values above 1, rarely encountered in Heather or Middle Jurassic samples. The upper Draupne Formation is also characterised by the presence of 17α(H),21β(H)-28,30-bisnorhopane which is commonly absent or only present in small amounts in the lower Draupne and Heather Formation (Fig. 12a). This was also observed by Kubala *et al*. (2003) in the East Shetland Basin, Ineson *et al*. (2003) in the Volgian to Ryazanian shales of the Danish Central Graben, and Justwan and Dahl (2005) in the Greater Balder area. The occurrence of this compound has been associated with anoxic environments (e.g. Grantham *et al*., 1980; Katz and Elrod, 1983; Peters and Moldowan, 1993), and its presence is a further indication of widespread anoxia in the upper Draupne Formation in addition to the Pr/Ph ratio and the ratio of C_{34} to C_{35} homohopanes.

The stratigraphic distribution of bisnorhopane in the South Viking Graben appears to be different from its distribution in the North Viking Graben as shown by Dahl (2004). In the Oseberg area, bisnorhopane is absent in the post-rift section of the Draupne Formation. Huc *et al*. (1985) also noted the absence of bisnorhopane in the "hot shales" in their study area. It is however important to note that elevated amounts of bisnorhopane were encountered in shales from the Middle Jurassic Hugin Formation in wells *16/7-2* and *15/9-18* (Fig. 11). Upper Jurassic samples show higher ratios of dia- versus regular steranes than Middle Jurassic samples, although it is difficult to differentiate between the Upper Jurassic sections.

The upper Draupne Formation has a narrow distribution of Pr/Ph ratio values with an average of 1.38, while the lower Draupne Formation shows a much broader distribution and a slightly higher average of 1.69. The Pr/Ph ratio decreases upwards within the Upper Jurassic up to genetic sequence C2 or the base of sequence D (*sensu* Fraser *et al*., 2003), where for most wells a change to increasing values can be observed (Fig. 7). This shift from decreasing to increasing values occurs, as mentioned before, approximately at the same time as the peak of the gamma-ray values. Considering all the analysed formations, a significant decrease in Pr/Ph ratio from the Middle Jurassic to the Upper Jurassic can be observed.

Regional and stratigraphic variations

The large variations in source facies and potential revealed by the mapping are also reflected by their molecular and isotopic characteristics. The amount of dispersion shows strong facies variations, and significant overlap in the ranges for geochemical parameters complicates the unambiguous identification of the source intervals. Interestingly, the variation in molecular properties is less pronounced in the post-rift upper Draupne Formation (Fig. 12). This is in agreement with the source rock potential maps presented earlier, suggesting a more uniform oil-prone facies in the upper Draupne Formation. The increasing dominance of C_{27} over C_{29} regular steranes upwards, as well as the trend towards lighter isotopic values upwards, the ratio of C_{30} moretane to C_{30} hopane and the predominance of low molecular weight alkanes up to C_{17} in the Draupne Formation, supports the conclusion that marine, oil-prone Type II material increases upwards in abundance. Another important conclusion is that the degree of oxygenation decreases upwards from the Middle Jurassic, as supported by Pr/Ph ratios, C_{34}/C_{35} homohopane ratios and the occurrence of bisnorhopane. Fig.12c shows the general decrease in Pr/Ph ratio upwards, and also the large variations in this parameter.

We tried to examine the significance of the variation by studying the geographical distribution of Pr/Ph ratio values as indices for anoxic conditions. In order to increase the number of data points for regional mapping, GC data from geochemical service reports were used as a supplement. Interlaboratory variation was regarded as insignificant for the Pr/Ph ratio. Average Pr/Ph ratios were mapped for the Heather, lower and upper Draupne Formations (Fig. 13). It can be observed that anoxic conditions spread in the

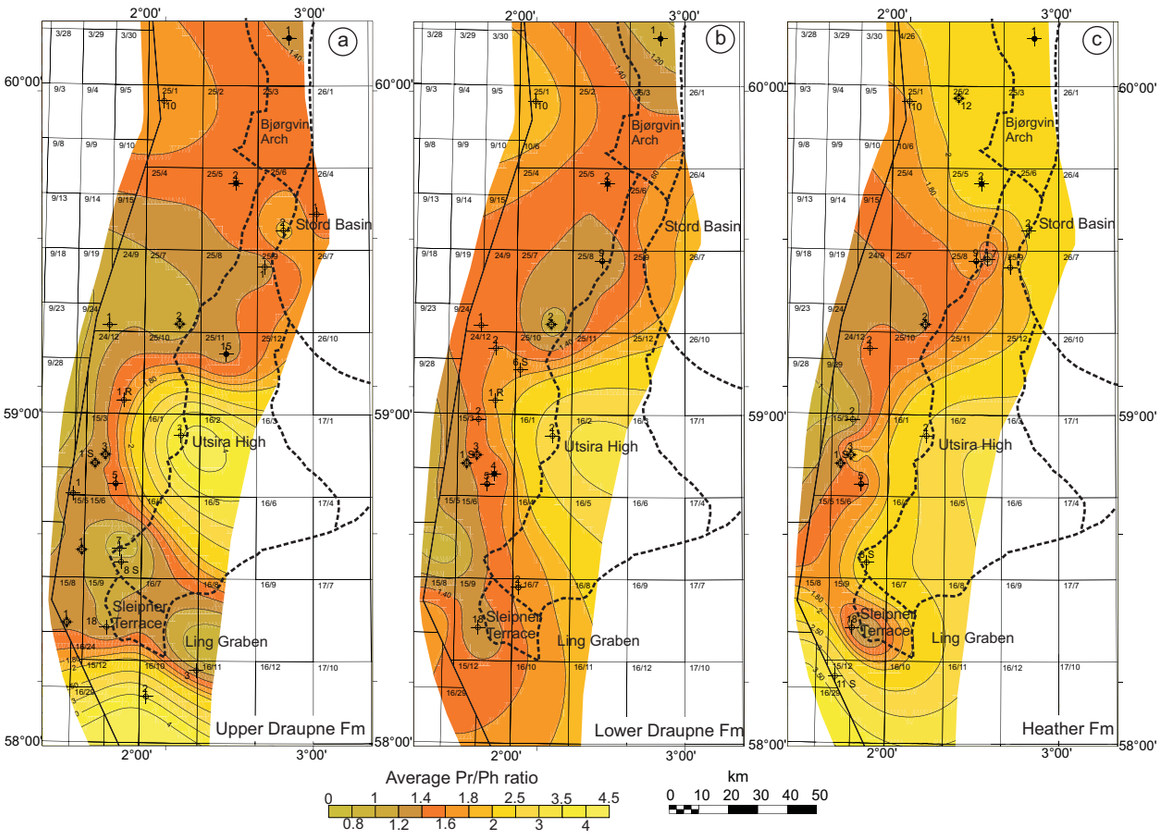

Fig. 13. Maps of average Pr/Ph ratios for (a) the upper Draupne (b) the lower Draupne and (c) the Heather Formation, contoured in IRAP using convergent trend gridding.
The large variation in individual values observed in the data set can here be interpreted in map view. Decreasing values upwards can be interpreted in terms of the spreading of anoxia in the area during the Late Jurassic transgression.

graben centre during the transgression in the Upper Jurassic from local patches in the Heather Formation (Fig. 13c) to a more continuous north-south oriented area in the lower Draupne Formation (Fig. 13b), to a generally anoxic graben system in the upper Draupne Formation (Fig.13a). Depositional conditions in the Utsira High in Blocks 25/11 and 16/1 appear to have been oxygenated throughout the Late Jurassic. The observations support the generally accepted model that the Upper Jurassic Draupne Formation was deposited in anoxic bottom waters; however, they demonstrate the development of anoxic conditions through time in the Viking Graben.

The data presented here support a model of water column stratification with gradual ascent of the O_2:H_2S interface. Such a mechanism was proposed on a smaller scale for the cycles in the Kimmeridge Clay Formation in the Wessex Basin by Tyson (1979). Conditions for source rock formation were most favourable during the mid-Volgian to Late Ryazanian when dysoxic to anoxic conditions were widely established in the South Viking Graben.

Controls on source potential and source facies distribution

As mentioned above, the source facies distribution of Jurassic source rocks in the South Viking Graben is controlled by a complex interplay of factors (Cooper *et al*., 1993), including platform width (Barnard *et al*., 1981), mass transport mechanisms (Huc *et al*., 1985), dilution effects (Justwan and Dahl, 2005) and preservation (Huc *et al*., 1985). Intensive mixing of different types of organic matter may have occurred in the fairly narrow graben, where terrestrial and reworked organic matter could have been transported from surrounding highs by mass flows.

In the following paragraphs, we attempt to highlight the influence of the various factors and to determine the most important control on source facies distribution in the Upper Jurassic source rock section. The crudeness of the methods used to determine the amount of oil- and gas-prone organic matter, and the fact that averages for bulk geochemical and molecular parameters as well as the linear sediment accumulation

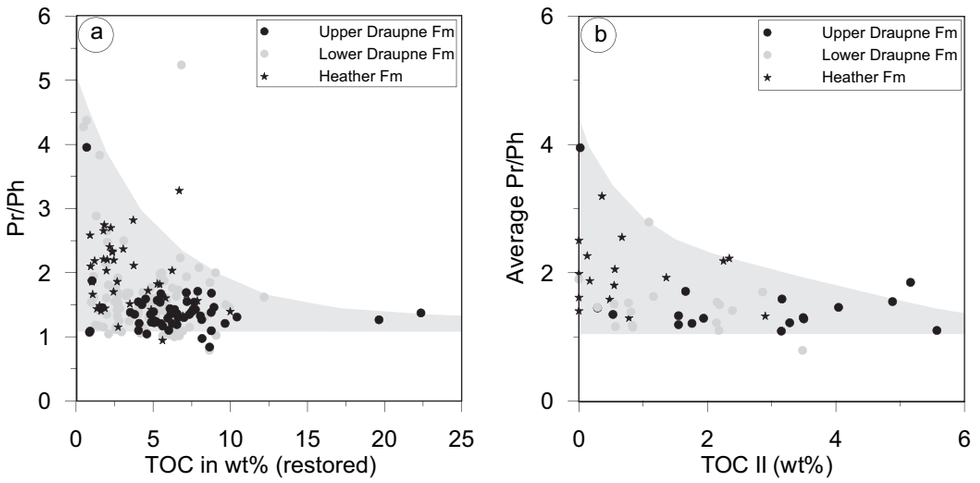

Fig. 14. Cross-plots of TOC and Pr/Ph ratios. (a) Measured Pr/Ph ratios and restored TOC for individual samples. (b) Average Pr/Ph ratios and TOCII (as shown on maps in Figs 9 and 13). The amount of oil-prone organic mater appears to increase with decreasing Pr/Ph ratios in the lower Draupne and Heather Formation. No direct relationship is evident in the upper Draupne Formation, low Pr/Ph values are common. This relation can be interpreted as an effect of increased preservation of organic matter in increasingly more anoxic environments.

rates were used, does not allow detailed discussion of productivity and organic matter accumulation models; however, the most significant controls on the facies can be determined.

The highest overall amount of organic matter can be observed in depocentres in the graben due to sediment focusing and sea-floor topography. Oil-prone organic matter, however, is not restricted to the basinal area, but occurs also on the flanks of the highs and even on the highs. One important example is the flank of the Stord Basin which shows high TOCII values.

Figs 8 and 9 illustrate the role of dilution by gas-prone and inert material on the source facies distribution. Average values for oil- and gas-prone TOC as well as inert organic matter show that organic matter capable of hydrocarbon generation is mixed in variable amounts with a near-constant input of inert organic matter; the maps of the lower Draupne Formation show that dilution of oil-prone material by gas-prone material locally plays an important role. The input of inert organic matter is higher in the vicinity of mass flow sands as was also observed by Tyson (1989). The absolute amount of gas-prone organic matter is fairly constant, with slightly elevated levels in the lower Draupne Formation indicating the influence of mass flows which transported large volumes of reworked and gas-prone organic matter from the East Shetland Platform and the Utsira High. As discussed earlier, the upper Draupne Formation shows a reduction in the proportion of gas-prone material. This is related to the decreased occurrence of mass flows and the generally decreased input of terrestrial organic matter. This reduced input of terrestrial organic matter is probably related to an arid climatic episode from the early Volgian to the late Ryazanian (c.f. Wignall and Ruffell, 1990).

Both absolute amount and proportion of oil-prone organic matter increase from the Heather to the upper Draupne Formation. This is supported by molecular data including C_{27} to C_{29} regular steranes and GC parameters. The oil-prone nature of the upper Draupne Formation must therefore be explained by factors other than reduced dilution by terrestrial and reworked organic matter (Justwan and Dahl, 2005).

The effect of anoxia on the preservation of organic matter was therefore evaluated. The increasing importance of anoxia from the Middle Jurassic to the upper Draupne Formation is shown by a series of factors including increasing Pr/Ph ratios, increasing relative amounts of bisnorhopane and C_{34}/C_{35} homohopane indices. Cross-plots of TOC and Pr/Ph indicate that TOC values increase with decreasing Pr/Ph ratios. Both plots of measured Pr/Ph ratios versus restored TOC values (Fig. 14a), as well as a plot of average Pr/Ph ratios versus TOCII values used in the mapping (Fig. 14b), show negative correlations. There is a stronger dependency of TOC and TOCII on the Pr/Ph ratio in the lower Draupne and Heather Formation. The large variation in TOC values in the upper Draupne Formation, however, cannot be attributed to variations in oxygenation, as anoxia is widespread from the Middle Volgian onwards.

In order to investigate further the cause of the variations in TOCII in the upper Draupne Formation, the relationship between the amount of oil-prone material and the average compacted linear sediment accumulation rate for the wells used in Fig. 9 was examined using a log-log cross-plot (Müller and Süss,

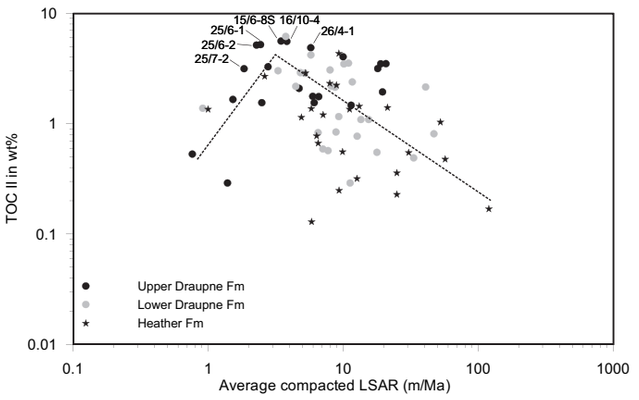

Fig. 15. Plot of average compacted linear sedimentation rates (LSAR) versus TOCII (log-log scale) for the upper and lower Draupne and Heather Formations. Values of oil-prone TOC increase with increasing LSAR up to an optimum value of 3 m/Ma and decrease thereafter due to siliciclastic dilution. Excellent oil potential in the upper Draupne Formation in wells *16/10-4*, *15/6-8S*, *25/6-1*, *25/6-2*, *26/4-1* and *25/7-2* is associated with sediment accumulation rates ideal for the preservation of organic matter.

1979). Sand intervals have been excluded and the durations used in the calculation have been taken from Esso's proprietary sequence stratigraphic famework using the timescale of Hardenbol *et al.* (1998). Full sequences without gaps have been assumed for simplification. Although not very pronounced, TOCII values increase up to a linear sediment accumulation rate of around 3 m/Ma and decrease from this point onwards with increasing rates due to siliciclastic dilution (Fig. 15). This phenomenon was previously described by Ibach (1982) using a large database of DSDP samples. Ibach however determined a much higher critical sedimentation rate of 40.8 m/Ma. The variations in the upper Draupne Formation's oil potential can thus be attributed to variations in siliciclastic dilution. The maxima on the flank of the Stord Basin in wells *25/6-1*, *25/6-2* and *26/4-1* and the southern edge of the Utsira High in well *15/6-8 S* were probably caused by reduced siliciclastic input at sedimentation rates ideal for the preservation of organic matter, and not (as previously proposed) by enhanced preservation in local pool-like areas with stagnant water (Justwan and Dahl, 2005). The lower Draupne and the Heather Formations have generally higher accumulation rates above the critical value, and show decreasing TOC values with increasing siliciclastic input (Fig.15). There is no correlation between TOCIV and linear sediment accumulation rate, but there is a weak positive correlation between TOC and linear sediment accumulation rate for the upper, lower Draupne and Heather Formations (not shown), indicating that a higher amount of gas-prone material is transported to the basin with higher siliciclastic input.

The source facies of the upper Draupne Formation therefore appears to be controlled principally by the reduced input of gas-prone organic matter, the generally good preservation in a widely anoxic environment, and the reduced siliciclastic dilution. The facies and potential of the lower Draupne Formation, on the other hand, appear to depend to a greater extent on dilution by reworked and gas-prone organic matter, derived by mass flow processes from surrounding highs. Preservation effects and siliciclastic dilution still play a role in the control on the facies distribution, but to a lesser degree than in the upper Draupne Formation. The degree of oxygenation and thus preservation, as well as the amount of siliciclastic dilution, are the key factors determining the facies of the Heather Formation. Dilution by gas-prone and reworked organic matter is only of local importance.

CONCLUSIONS

(1) The upper section of the Draupne Formation of mid-Volgian to Ryazanian age is up to 330 m thick in the South Viking Graben, and represents a post-rift clay drape deposited with low sediment accumulation rates averaging 7 m/Ma in the analysed wells. The syn-rift section of Oxfordian to mid-Volgian age is up to 1,600 m thick in the graben centre and has a higher average linear sediment accumulation rate of 12 m/Ma in the analysed wells. The up to 930 m thick Heather Formation was deposited more rapidly than the Draupne Formation (20 m/Ma on average, in the analysed wells).

(2) The mid-Volgian section is characterised by a basin-wide peak in gamma-ray values. This peak coincides with a shift in the trend of Pr/Ph ratio and the transition from syn- to post-rift sedimentation; it can therefore be used to divide the Upper Jurassic section where sequence stratigraphic or biostratigraphic data are not available.

(3) The top of the oil window for the Upper Jurassic source rock section from Rock-Eval and

vitrinite reflectance data occurs at 3,500 m, while the Middle Jurassic source rocks enter the oil window at around 3,800 m. Significant expulsion of hydrocarbons occurs at approximately 4,000 m from the upper Draupne Formation, and at 4,100 m and 4,200 m, respectively, from the lower Draupne and Heather Formations.

(4) Quantitative oil- and gas-potential maps based on maturity-corrected Rock-Eval data point to the very high oil potential for the thin upper Draupne Formation with maxima on the southern flank of the Utsira High and the flank of the Stord Basin. This is not consistent with previous assumptions that oil potential on highs and flanks is reduced. The lower Draupne Formation has predominantly gas potential, with the strong influence of mass flow processes which transported gas-prone and inert organic matter to the deep basin. The gas potential of all sections decreases to the east, suggesting the main sediment source was the East Shetland Platform. The Heather Formation is the least oil-prone section and exhibits mainly gas potential.

(5) Source potential and molecular and isotopic properties show major variations in the Middle to Upper Jurassic section. Biomarker and isotope data indicate changes in depositional environment from the Middle Jurassic to the upper Draupne Formation which support the results of Rock-Eval data.

(6) Decreasing Pr/Ph ratios, decreasing dominance of C_{34} homohopanes over C_{35} homohopanes as well as increasing relative amounts of 17α(H),21β(H)-28,30-bisnorhopane indicate a decreasing degree of oxygenation from the Heather to the upper Draupne Formation. Maps of the Pr/Ph ratio show that this development is consistent with a permanently stratified water column with an ascending O_2:H_2S interface.

(7) The distribution of organofacies and source potential in the South Viking Graben is the result of the interplay of factors including siliciclastic dilution, dilution by gas-prone and inert material, preservation and basin geometry. The highest overall TOC values are encountered in depocentres in the graben, and the narrow shape of the graben allowed terrestrial and reworked organic matter to reach the graben centre from the surrounding highs on both eastern and western flanks. While the source facies of the upper Draupne Formation is controlled by preservation under anoxic to dysoxic conditions together with reduced dilution by siliciclastic, terrestrial and reworked material, that in the lower Draupne is mainly controlled by dilution by terrestrial and reworked organic matter transported by mass flows. The Heather Formation's facies can be explained by siliciclastic dilution and preservation effects. The exceptionally high oil potential in the upper Draupne Formation on the flank of the Stord Basin and the Utsira High is related to deposition under sedimentation rates promoting preservation of organic matter.

ACKNOWLEDGEMENTS

Financial support for this project was provided by Esso Exploration and Production Norway A/S and the Research Council of Norway (Grant *NFR 157825/432*). We are indebted to Norsk Hydro A/S for the Rock-Eval analyses. Jørgen Bojesen-Koefoed and Peter Nytoft at GEUS (Denmark) are thanked for the use of the MPLC system and technical assistance in the laboratory. The authors would also like to thank the Norwegian Petroleum Directorate for the release of sample material, and Esso Exploration and Production Norway A/S for all the data received and valuable technical discussions. Aurélie Nowinski is thanked for fruitful comments on earlier versions of the manuscript. Reviews by Iain Scotchman and Richard Tyson on a previous version of the manuscript are acknowledged with thanks.

REFERENCES

BAIRD, R.A., 1986. Maturation and source rock evaluation of Kimmeridge Clay, Norwegian North Sea. *AAPG Bull.*, **70**, 1-11.

BARNARD, P.C., COLLINS, A.G., and B.S. COOPER, B.S., 1981. Identification and distribution of kerogen facies in a source rock horizon - examples from the North Sea basin, In: BROOKS, J. (Ed.), Organic maturation studies and fossil fuel exploration. Academic Press, London, 271-282.

BARNARD, P.C. and COOPER, B.S., 1981. Oils and source rocks of the North Sea area. In: ILLING, L.V. and HOBSON, G.D. (Eds), Petroleum geology of the continental shelf of North-West Europe: Proceedings of the 2nd Conference. Heyden and Son, London, 169-175.

BRASSELL, S.C., EGLINTON, G. and HOWELL, V.J., 1987. Palaeoenvironmental assessment for marine organic-rich sediments using molecular organic geochemistry. In: BROOKS, J. and FLEET, A.J. (Eds), Marine petroleum source rocks. *Geol. Soc. London Spec. Publ.,* **26**, 79-98.

BRAY, E.E. and EVANS, E.D., 1961. Distribution of n-paraffins as a clue to recognition of source beds. *Geochim. Cosmochim. Acta,* **22**, 2-15.

BROOKS, J.D., GOULD, K. and SMITH, J.W., 1969. Isoprenoid hydrocarbons in coal and petroleum. *Nature*, **222**, 257-259.

COCKINGS, J.H., KESSLER, L.G., MAZZA, T.A. and RILEY, L.A., 1992. Bathonian to mid-Oxfordian sequence stratigraphy of the South Viking Graben, North Sea. In: HARDMAN, R.F.P. (Ed.), Exploration Britain; geological insights for the next decade. *Geol. Soc. London Spec. Publ.*, **67**, 65-105.

COOPER, B.S. and BARNARD, P.C., 1984. Source rock and oils of the central and northern North Sea. In: DEMAISON, G. and MURRIS ROELEF, J. (Eds), Petroleum geochemistry and basin evaluation. *AAPG Memoir*, **35**, 303-314.

COOPER, B.S., BARNARD, P.C. and TELNAES, N., 1993. The Kimmeridge Clay Formation of the North Sea. In: BROOKS, J. and FLEET, A.J. (Eds), Marine petroleum source rocks. *Geol. Soc. London Spec. Publ.*, **26**, 89-110.

CORNFORD, C., 1998. Source rocks and hydrocarbons of the North Sea. In: GLENNIE, K.W. (Ed.), Petroleum geology

of the North Sea; basic concepts and recent advances. Blackwell, Oxford, 376-462.

CORNFORD, C., GARDNER, P. and BURGESS, C., 1998. Geochemical truths in large data sets; I, Geochemical screening data. *Org. Geochem*., **29**, 519-530.

DAHL, B., 2004. The use of bisnorhopane as a stratigraphic marker in the Oseberg Back Basin, North Viking Graben, Norwegian North Sea. *Org. Geochem*., **35**, 1551-1571.

DAHL, B., BOJESEN-KOEFOED, J., HOLM, A., JUSTWAN, H., RASMUSSEN, E. and THOMSEN, E., 2004. A new approach to interpreting Rock-Eval S2 and TOC data for kerogen quality assessment. *Org. Geochem*., **35**, 1461-1477.

DAHL, B. and SPEERS, G.C., 1985. Organic Geochemistry of the Oseberg Field (I). In: THOMAS, B.M., DORE, A.G., EGGEN, S.S., HOME, P.C. and LARSEN, R.M. (Eds), Petroleum geochemistry in exploration of the Norwegian Shelf. Graham and Trotman, London, 185-195.

DEMAISON, G.J. and MOORE, G.T., 1980. Anoxic environments and oil source bed genesis. *AAPG Bull*., **64**, 1179-1209.

di PRIMIO, R., 2002. Unraveling secondary migration effects through the regional evaluation of PVT data; a case study from Quadrant 25, NOCS. *Org. Geochem*., **33**, 643-653.

DIDYK, B.M., SIMONEIT, B.R.T., BRASSELL, S.C. and EGLINTON, G., 1978. Organic geochemical indicators of palaeoenvironmental conditions of sedimentation. *Nature*, **272**, 216-222.

DIECKMANN, V., FOWLER, M. and HORSFIELD, B., 2004. Predicting the composition of natural gas generated by the Duvernay Formation (Western Canada Sedimentary Basin) using a compositional kinetic approach. *Org. Geochem*., **35**, 845-862.

DORE, A.G., VOLLSET, J. and HAMAR, G.P., 1985. Correlation of the offshore sequences referred to the Kimmeridge Clay Formation; relevance to the Norwegian sector. In: THOMAS, B.M., DORE, A.G., EGGEN, S.S., HOME, P.C. and LARSEN, R.M. (Eds), Petroleum geochemistry in exploration of the Norwegian Shelf. Graham and Trotman, London, 27-37.

ESPITALIE, J., 1987. Organic Geochemistry of the Paris Basin. In: BROOKS, J. and GLENNIE, K.W. (Eds), Petroleum geology of Northwest Europe. Graham and Trotman, London, 71-86.

FAERSETH, R.B., 1996. Interaction of Permo-Triassic and Jurassic extensional fault-blocks during the development of the northern North Sea. *Journ. Geol. Soc. London*, **153**, 931-944.

FIELD, J.D., 1985. Organic geochemistry in exploration of the northern North Sea. In: THOMAS, B.M., DORE, A.G., EGGEN, S.S., HOME, P.C. and LARSEN, R.M. (Eds), Petroleum geochemistry in exploration of the Norwegian Shelf. Graham and Trotman, London, 39-57.

FISHER, M.J. and MILES, J.A., 1983. Kerogen types, organic maturation and hydrocarbon occurrences in the Moray Firth and South Viking Graben, North Sea basin. In: BROOKS, J. (Ed.), Petroleum geochemistry and exploration of Europe. *Geol. Soc. London Spec. Publ*., **12**, 195-201.

FISHER, M.J. and MUDGE, D.C., 1998. Triassic. In: GLENNIE, K.W. (Ed.), Petroleum geology of the North Sea; basic concepts and recent advances. Blackwell, Oxford, 212-244.

FRASER, S.I., ROBINSON, A.M., JOHNSON, H.D., UNDERHILL, J.R., KADOLSKY, D.G.A., CONNELL, R., JOHANNESSEN, E.P. and RAVNAS, R., 2003. Upper Jurassic. In: EVANS, D., GRAHAM, C., ARMOUR, A. and BATHURST, P. (Eds), The Millennium Atlas: petroleum geology of the central and northern North Sea. Geol. Soc. London, 289-316.

GABRIELSEN, R.H., KYRKJEBØ, R., FALEIDE, J.I., FJELDSKAAR, W. and KJENNERUD, T., 2001. The Cretaceous post-rift basin configuration of the northern North Sea. *Petroleum Geoscience*, **7**, 137-154.

GELPI, E., SCHNEIDER, H., MANN, J. and ORO, J., 1970. Hydrocarbons of geochemical significance in microscopic algae. *Phytochemistry,* **9**, 603-612.

GOFF, J.C., 1983. Hydrocarbon generation and migration from Jurassic source rocks in the E Shetland Basin and Viking Graben of the northern North Sea. *Journ. Geol. Soc. London*, **140**, 445-474.

GORMLY, J.R., BUCK, S.P. and CHUNG, H.M., 1994. Oil-source rock correlation in the North Viking Graben. *Org. Geochem*., **22**, 403-413.

GRANTHAM, P.J., POSTHUMA, J. and DE GROOT, K., 1980. Variation and significance of the C-27 and C-28 triterpane content of a North Sea core and various North Sea crude oils. *Physics and Chemistry of the Earth*, **12**, 29-38.

GREGERSEN, U., MICHELSEN, O. and SØRENSEN, J.C., 1997. Stratigraphy and facies distribution of the Utsira Formation and the Pliocene sequences in the northern North Sea. *Mar. Petrol. Geol*., **14**, 893-914.

HALLAM, A. and BRADSHAW, M.J., 1979. Bituminous shales and oolitic ironstones as indicators of transgressions and regressions. *Journ. Geol. Soc. London*, **136**, 157-164.

HANSLIEN, S., 1987. Balder. In: SPENCER, A.M. (Ed.), Geology of the Norwegian oil and gas fields. Graham and Trotman, Norwell, 193-201.

HARDENBOL, J., THIERRY, J., FARLEY, M.B., DE GRACIANSKY, P.C. and VAIL, P.R., 1998. Mesozoic and Cenozoic sequence chronostratigraphic framework of European basins In: Mesozoic and Cenozoic sequence stratigraphy of European basins. *SEPM Spec. Publ*., **60**, 3-13.

HUANG, W.Y. and MEINSCHEIN, W.G., 1979. Sterols as ecological indicators. *Geochim. Cosmochim. Acta*, **43**, 739-746.

HUC, A.Y., 1988. Aspects of depositional processes of organic matter in sedimentary basins. *Org. Geochem*., **13**, 263-272.

HUC, A.Y., 1990. Understanding organic facies; a key to improved quantitative petroleum evaluation of sedimentary basins. In: HUC, A.Y. (Ed.), Deposition of organic facies. *AAPG Studies in Geol*., **30**, 1-11.

HUC, A.Y., IRWIN, H. and SCHOELL, M., 1985. Organic matter quality changes in an Upper Jurassic shale sequence from the Viking Graben. In: THOMAS, B.M., DORE, A.G., EGGEN, S.S., HOME, P.C. and LARSEN, R.M. (Eds), Petroleum geochemistry in exploration of the Norwegian Shelf. Graham and Trotman, London, 179-183.

HUSMO, T., HAMAR, G.P., HØILAND, O., JOHANNESSEN, E.P., RØMULD, A., SPENCER, A.M. and TITTERTON, R., 2003. Lower and Middle Jurassic. In: EVANS, D., GRAHAM, C., ARMOUR, A. and BATHURST, P. (Eds), The Millennium Atlas: petroleum geology of the central and northern North Sea. Geol. Soc. London, 129-156.

IBACH, L.E.J., 1982. Relationship between sedimentation rate and total organic carbon content in ancient marine sediments. *AAPG Bull*., **66**, 170-188.

INESON, J.R., BOJESEN-KOEFOED, J.A., DYBKJAER, K. and NIELSEN, L.H., 2003. Volgian-Ryazanian "hot shales" of the Bo Member (Farsund Formation) in the Danish Central Graben, North Sea; stratigraphy, facies and geochemistry. In: INESON, J.R. and SURLYK, F. (Eds), The Jurassic of Denmark and Greenland. *Geological Survey of Denmark and Greenland Bulletin*, **1**, 403-436.

ISAKSEN, G.H. and BOHACS, K.M., 1995. Geological controls of source rock geochemistry through relative sea level; Triassic, Barents Sea. In: KATZ, B.J. (Ed.), Petroleum Source Rocks. Springer, Berlin, 25-50.

ISAKSEN, G.H., CURRY, D.J., YEAKEL, J.D. and JENSSEN, A.I., 1998. Controls on the oil and gas potential of humic coals. *Org. Geochem*., **29**, 23-44.

ISAKSEN, G.H. and LEDJE, K.H.I., 2001. Source rock quality and hydrocarbon migration pathways within the greater Utsira High area, Viking Graben, Norwegian North Sea.

AAPG Bull., **85**, 861-883.
ISAKSEN, G.H., PATIENCE, R., VAN GRAAS, G. and JENSSEN, A.I., 2002. Petroleum system analysis in a rift basin with mixed marine and nonmarine source rocks; the South Viking Graben, North Sea. *AAPG Bull*., **86**, 557-591.
JACQUIN, T., DARDEAU, G., DURLET, C., DE GRACIANSKY, P.C. and HANTZPERGUE, P., 1998. The North Sea cycle; an overview of 2nd-order transgressive/ regressive facies cycles in Western Europe. In: Mesozoic and Cenozoic sequence stratigraphy of European basins. *SEPM Spec. Publ*., **60**, 445-466.
JUSTWAN, H. and DAHL, B., 2005. Quantitative Hydrocarbon Potential Mapping and Organofacies Study in the Greater Balder Area, Norwegian North Sea. In: DORE, A.G. and VINING, B.A. (Ed.), Petroleum Geology: of North-West Europe and Global Perspectives Proceedings of the 6th Petroleum Geology Conference. Geol. Soc. London, 1317-1329.
KATZ, B.J. and ELROD, L.W., 1983. Organic Geochemistry of DSDP Site 467, offshore California, middle Miocene to lower Pliocene strata. *Geochim. Cosmochim. Acta*, **47**, 389-396.
KUBALA, M., BASTOW, M., THOMPSON, S., SCOTCHMAN, I. and ØYGARD, K., 2003. Geothermal regime, petroleum generation and migration. In: EVANS, D., GRAHAM, C., ARMOUR, A. and BATHURST, P. (Eds), The Millennium Atlas: petroleum geology of the central and northern North Sea. Geol. Soc. London, 289-315.
MILLER, R.G., 1990. A paleoceanographic approach to the Kimmeridge Clay Formation. In: HUC, A.Y. (Ed.), Deposition of organic facies. *AAPG Studies in Geol*., **30**, 13-26.
MÜLLER, P.J. and SÜSS, E., 1979. Productivity, sedimentation rate, and sedimentary organic matter in the oceans; I, Organic carbon preservation. *Deep-Sea Research*, **26**, 1347-1362.
NORTHAM, M.A., 1985. Correlation of northern North Sea oils; the different facies of their Jurassic source. In: THOMAS, B.M., DORE, A.G., EGGEN, S.S., HOME, P.C. and LARSEN, R.M. (Eds), Petroleum geochemistry in exploration of the Norwegian Shelf. Graham and Trotman, London, 93-99.
NORWEGIAN PETROLEUM DIRECTORATE, 2005. Factmaps. [22 May 2005]. Available at: <http://217.68.117.237/website/NPDGIS/viewer.htm>.
OSCHMANN, W., 1988. Kimmeridge clay sedimentation; a new cyclic model. *Palaeogeography, Palaeoclimatology, Palaeoecology*, **65**, 217-251.
PARRISH, J.T. and CURTIS, R.L., 1982. Atmospheric circulation, upwelling, and organic-rich rocks in the Mesozoic and Cenozoic eras. Paleogeography and Climate. Elsevier, Amsterdam, 31-66.
PETERS, K.E. and MOLDOWAN, J.M., 1991. Effects of source, thermal maturity, and biodegradation on the distribution and isomerization of homohopanes in petroleum. *Org. Geochem*., **17**, 47-61.
PETERS, K.E. and MOLDOWAN, J.M., 1993. The biomarker guide; interpreting molecular fossils in petroleum and ancient sediments. Prentice Hall, Englewood Cliffs, 363 pp.
PETERSEN, H.I., BOJESEN-KOEFOED, J.A. and NYTOFT, H.P., 2002. Source rock evaluation of Middle Jurassic coals, Northeast Greenland, by artificial maturation; aspects of petroleum generation from coal. *AAPG Bull*., **86**, 233-256.
RADKE, M., WILLSCH, H. and WELTE, D.H., 1980. Preparative hydrocarbon determination by automated Medium Pressure Liquid Chromatography. *Analytical Chemistry*, **52**, 406-411.
RAMANAMPISOA, L. and DISNAR, J.R., 1994. Primary control of paleoproduction on organic matter preservation and accumulation in the Kimmeridge rocks of Yorkshire (UK). *Org. Geochem*., **21**, 1153-1167.
RATTEY, R.P. and HAYWARD, A.B., 1993. Sequence stratigraphy of a failed rift system; the Middle Jurassic to Early Cretaceous basin evolution of the central and northern North Sea. In: PARKER, J.R. (Ed.), Petroleum geology of Northwest Europe: Proceedings of the 4th conference. Geol. Soc. London, 215-249.
RAWSON, P.F. and RILEY, L.A., 1982. Latest Jurassic-Early Cretaceous events and the "late Cimmerian unconformity" in North Sea area. *AAPG Bull*., **66**, 2628-2648.
SCOTCHMAN, I.C., 1991. Kerogen facies and maturity of the Kimmeridge clay formation in southern and eastern England. *Mar. Petrol. Geol*., **8**, 278-295.
SEIFERT, W.K. and MOLDOWAN, J.M., 1985. Paleoreconstruction by biological markers. In: Proceedings of the Annual Convention - Indonesian Petroleum Association, 189-212.
SEIFERT, W.K. and MOLDOWAN, J.M., 1986. Use of biological markers in petroleum exploration. *Methods in Geochemistry and Geophysics*, **24**, 261-290.
SKARPNES, O., HAMAR, G.P., JAKOBSSON, K.H. and ORMAASEN, D.E., 1980. Regional Jurassic setting of the North Sea north of the Central Highs. In: The sedimentation of the North Sea reservoir rocks. NPF, Oslo, 8.
SNEIDER, J.S., DE CLARENS, P. and VAIL, P.R., 1995. Sequence stratigraphy of the Middle to Upper Jurassic, Viking Graben, North Sea. In: STEEL, R.J. (Ed.), Sequence Stratigraphy on the Northwest European Margin. *NPF Special Publication*, **5**, 167-197.
TEN HAVEN, H.L., DE LEEUW, J.W., RULLKOETTER, J. and SINNINGHE-DAMSTE, J.S., 1987. Restricted utility of the pristane/phytane ratio as a palaeoenvironmental indicator. *Nature*, **330**, 641-643.
THOMAS, B.M., MØLLER-PEDERSEN, P., WHITAKER, M.F. and SHAW, N.D., 1985. Organic facies and hydrocarbon distributions in the Norwegian North Sea. In: THOMAS, B.M., DORE, A.G., EGGEN, S.S., HOME, P.C. and LARSEN, R.M. (Eds), Petroleum geochemistry in exploration of the Norwegian Shelf. Graham and Trotman, London, 3-26.
TISSOT, B.P. and WELTE, D.H., 1984. Petroleum formation and occurrence. Springer, Berlin, 699 pp.
TYSON, R.V. 1989. Late Jurassic palynofacies trends, Piper and Kimmeridge Clay Formations, UK onshore and northern North Sea. In: BATTEN, D.J. and KEEN, M. (Eds), Northwest European Micropalaeontology and Palynology. British Micropalaeontological Society Series, Ellis Horwood, Chichester, 135-172.
TYSON, R.V., 2004. Variation in marine total organic carbon through the type Kimmeridge Clay Formation (Late Jurassic), Dorset, UK. *Journ. Geol. Soc. London*, **161**, 667-673.
TYSON, R.V., WILSON, R.C.L. and DOWNIE, C., 1979. A stratified water column environmental model for the type Kimmeridge Clay. *Nature*, **277**, 377-380.
UNDERHILL, J.R., 1998. Jurassic. In: GLENNIE, K.W. (Ed.), Petroleum geology of the North Sea; basic concepts and recent advances. Blackwell, Oxford, 245-292.
VOLLSET, J. and DORE, A.G., 1984. A revised Triassic and Jurassic Lithostratigraphic Nomenclature of the Norwegian North Sea. *Norwegian Petroleum Directorate Bull*., **59**, 53 pp.
WAPLES, D.W. and MARZI, R.W., 1998. The universality of the relationship between vitrinite reflectance and transformation ratio. *Org. Geochem*., **28**, 383-388.
WEISS, H.M., WILHELMS, A., MILLS, N., SCOTCHMER, J., HALL, P.B., LIND, K. and BREKKE, T., 2000. NIGOGA: The Norwegian Guide to Organic Geochemical Analyses. [22 Oct. 2004]. Available at: <http://www.npd.no/engelsk/nigoga/default.htm>.
WIGNALL, P.B., 1994. Black shales. Oxford University Press, Oxford, 127 pp.

WIGNALL, P.B. and RUFFELL, A.H., 1990. The influence of a sudden climatic change on marine deposition in the Kimmeridgian of Northwest Europe. *Journ. Geol. Soc. London*, **147**, 365-371.

ZIEGLER, P.A., 1992. North Sea rift system. *Tectonophysics*, **208**, 55-75.